ies have shown that adiponectin stimulates fatty acid oxidation in the skeletal muscle and inhibits glucose production in the liver by activating AMP-activated protein kinase (AMPK)[2] (26–29). We also reported that pioglitazone may induce amelioration of insulin resistance and diabetes via an adiponectin-dependent mechanism in the liver and an adiponectin-independent mechanism in the skeletal muscle (30).

Rimonabant has been shown to increase the plasma adiponectin levels in animal models of obesity and diabetes as well as in both diabetic and nondiabetic subjects (15, 31, 32). The results of the RIO-Lipids study provided evidence of a weight loss-independent effect of rimonabant on the plasma adiponectin levels (15). Furthermore, the metabolic improvements induced by rimonabant could be attributed, at least in part, to a moderate but significant increase in the plasma circulating adiponectin levels (15). However, whether the rimonabant-induced increase in the plasma levels of adiponectin might be causally involved in the effects of rimonabant, in particular its insulin-sensitizing effects, has not been addressed experimentally.

To address this issue, in the present study, we used *adipo*(−/−)ob/ob mice (30) to investigate whether rimonabant might be capable of ameliorating insulin resistance in the absence of adiponectin. We found that rimonabant significantly decreased the body weight and food intake to similar degrees in the ob/ob and *adipo*(−/−)ob/ob mice. Furthermore, we found significant amelioration of the insulin resistance in the ob/ob mice, in association with significant up-regulation of the serum adiponectin levels after 21 days of treatment with rimonabant at 30 mg/kg, body weight. The amelioration of insulin resistance in the ob/ob mice was attributed to the decrease of glucose production and activation of AMPK in the liver but not the increased glucose uptake by the skeletal muscle, induced by the drug. Interestingly, insulin resistance was also significantly, although only partially, improved in the *adipo*(−/−)ob/ob mice. Thus, the results suggest that rimonabant ameliorates insulin resistance via both adiponectin-dependent and adiponectin-independent pathways.

EXPERIMENTAL PROCEDURES

Animals and Genotyping—The mice were housed under a 12-h light/dark cycle and fed standard chow, CE-2 (CLEA Japan Inc., Tokyo, Japan). The composition of the chow was as follows: 25.6% (w/w) protein, 3.8% fiber, 6.9% ash, 50.5% carbohydrates, 4% fat, and 9.2% water. Ob/ob and *adipo*(−/−)ob/ob mice were generated by intercrossing *adipo*(+/−)ob/+ mice. All the mice were maintained on a C57Bl/6 background (30). All of the experiments in this study were conducted on 16–20-week-old male littermates. The animal care and experimental procedures were approved by the Animal Care Committee of the University of Tokyo.

Rimonabant Treatment Study—Rimonabant (SR141716) or vehicle (0.1% Tween 80 in saline) was administered to ob/ob and *adipo*(−/−)ob/ob mice at a dose of 30 mg/kg body weight by oral gavage, once daily for 21 consecutive days. Rimonabant was kindly provided by Sanofi-Aventis (Montpellier, France). We measured the body weights and food intake of the mice once daily for 21 consecutive days.

Hyperinsulinemic-Euglycemic Clamp Study—Clamp studies were carried out as described previously (30) with slight modifications. In brief, 2 days before the study, an infusion catheter was inserted into the right jugular vein under general anesthesia induced by sodium pentobarbital. Studies were performed on the mice under conscious and unstressed conditions after 8 h of fasting. A primed continuous infusion of insulin (Humulin R; Lilly) was administered (25.0 milliunits/kg/min), and the blood glucose concentration, monitored every 5 min, was maintained at 100–130 mg/dl by administration of glucose (5 g of glucose/10 ml enriched to ~20% with [6,6-$^2H_2$]glucose (Sigma)) for 120 min. Blood was sampled via tail tip bleeds at 90, 105, and 120 min for determination of the rate of glucose disappearance (R_d). R_d was calculated according to nonsteady-state equations (30), and endogenous glucose production was calculated as the difference between the R_d and the exogenous glucose infusion rate (30).

Western Blot Analysis—Tissues were excised and homogenized in ice-cold buffer A (25 mM Tris-HCl (pH 7.4), 10 mM sodium orthovanadate, 10 mM sodium pyrophosphate, 100 mM sodium fluoride, 10 mM EDTA, 10 mM EGTA, and 1 mM phenylmethylsulfonyl fluoride). The sample buffer for analysis under reducing conditions was composed of 3% SDS, 50 mM Tris-HCl (pH 6.8), 5% 2-mercaptoethanol, and 10% glycerol. Samples were mixed with 5× sample buffer, heated at 95 °C for 5 min for heat denaturation, separated on polyacrylamide gels, and then transferred to a Hybond-P polyvinylidene difluoride transfer membrane (Amersham Biosciences). Bands were detected with ECL detection reagents (Amersham Biosciences). To examine the Akt and AMPK phosphorylation and protein levels, lysates of liver and muscle were analyzed using anti-phospho-Akt (Cell Signaling Technology, Inc., Beverly, MA), anti-Akt (Cell Signaling Technology, Inc.) antibody, anti-phospho-AMPK (Cell Signaling Technology, Inc., Beverly, MA), and anti-AMPK (Cell Signaling Technology, Inc.) antibodies. For the analysis under nonreducing conditions, 2-mercaptoethanol was excluded from the sample buffer described above. To examine the isoforms of adiponectin, the serum samples were diluted 20-fold. Anti-mouse adiponectin antiserum was obtained by immunizing rabbits with the globular domain of mouse recombinant adiponectin produced in *Escherichia coli* (21).

Tissue Sampling for Insulin Signaling Pathway Study—Mice were anesthetized after 16 h of starvation, and 0.05 unit of human insulin (Humulin R; Lilly) was injected into the inferior vena cava. After 5 min, the liver was removed, and the specimens were used for protein extraction as described above.

Plasma Adiponectin and Lipid Measurements—The mice were deprived of access to food for 16 h before the measurements. The plasma adiponectin levels were determined with a mouse adiponectin enzyme-linked immunosorbent assay kit (Otsuka Pharmaceutical Co., Ltd., Tokyo, Japan). Serum triglyceride and free fatty acids (Wako Pure Chemical Industries Ltd., Osaka, Japan) were assayed by enzymatic methods.

[2] The abbreviations used are: AMPK, AMP-activated protein kinase; PEPCK, phosphoenolpyruvate carboxykinase; WAT, white adipose tissue; TG, triglyceride; FFA, free fatty acid; HMW, high molecular weight.

Measurement of Adipocyte Size—Epididymal white adipose tissue and subcutaneous fat were routinely processed for paraffin embedding, and 4-μm sections were cut and mounted on silanized slides. The adipose tissue sections were stained with hematoxylin and eosin, and the total adipocyte area was manually traced and analyzed using the Win ROOF software (Mitani Co. Ltd., Chiba, Japan). The white adipocyte area was measured in 200 or more cells/mouse in each group, in accordance with a previously described method (30), with slight modifications.

Oil Red O Staining and Quantification—Lipid accumulation was assessed by Oil Red O staining in 6-μm frozen sections of the liver fixed in phosphate-buffered 4% paraformaldehyde, according to a previously described method (33) with slight modification. In brief, the livers were washed once for 1 min with H_2O. After an additional wash for 1 min with 60% isopropyl alcohol, the livers were stained for 10 min at 37 °C with freshly diluted Oil Red O solution (6 parts of Oil Red O stock solution and 4 parts of H_2O; the Oil Red O stock solution contained 0.5% Oil Red O in isopropyl alcohol). After one wash for 2 min with 60% isopropyl alcohol and one wash for 1 min with H_2O, the livers were stained for 5 min with hematoxylin. The stain was then washed off with running water, and the silanized slides were stained. Oil Red O staining was quantified on digital images. Color images were acquired with a Nikon digital camera and analyzed using the Image J software. The percentage of the area of Oil Red O staining was measured from 9–10 different sections/mouse in each experimental group. Values were expressed as percentage of area.

Analysis of O_2 Consumption—Oxygen consumption was measured every 3 min for 24 h in the fasting mice using an O_2/CO_2 metabolism measurement device (model MK-5000; Muromachikikai, Tokyo, Japan). After rimonabant treatment for 21 days, each mouse was placed in a sealed chamber (560-ml volume) with an air flow rate of 500 ml/min at room temperature. The amount of oxygen consumed was converted to ml/min by multiplying it with the flow rate.

RNA Preparation and Taqman PCR—Total RNA was extracted from various tissues *in vivo* with TRIzol reagent (Invitrogen), in accordance with the manufacturer's instructions. After treatment with RQ1 RNase-free DNase (Promega, Madison, WI) to remove genomic DNA, cDNA was synthesized with MultiScribe reverse transcriptase (Applied Biosystems, Foster City, CA). Total RNA was prepared from 3T3L1 cells *in vitro* with an RNeasy Mini Kit (Qiagen Co., Düsseldorf, Germany), in accordance with the manufacturer's instructions. mRNA levels were quantitatively analyzed by fluorescence-based reverse transcriptase-PCR. The reverse transcription mixture was amplified with specific primers using an ABI Prism 7000 sequence detector equipped with a thermocycler. The primers used for MCP-1 (monocyte chemoattractant protein-1), resistin, phosphoenolpyruvate carboxykinase (PEPCK), carnitine palmitoyltransferase-1A, the hepatic isoform of carnitine palmitoyltransferase-1, protein phosphatase 2C, and cyclophilin were purchased from Applied Biosystems (Foster City, CA). The relative expression levels were compared by normalization to the expression levels of cyclophilin.

Cell Culture and Differentiation of 3T3L1 Adipocytes and Rimonabant Treatment—3T3L1 preadipocytes were cultured in Dulbecco's modified Eagle's medium containing 25 mM glucose and 10% fetal bovine serum at 37 °C. Confluent cultures were induced to differentiate into adipocytes by incubation in Dulbecco's modified Eagle's medium containing 25 mM glucose, 10% fetal bovine serum, 0.25 units/ml insulin, 0.25 μM dexamethasone, and 0.5 mM isobutyl-1-methylxanthine. After 2 days, the medium was changed to Dulbecco's modified Eagle's medium containing 25 mM glucose, 10% fetal bovine serum, and 0.025 units/ml insulin. All studies were performed on adipocytes 10 days after the initiation of differentiation (Day 0). Rimonabant treatment (100 nM and 1 μM) was started on Day 0, and DMSO was used as the vehicle. Prior to the start of the experiments, the differentiated adipocytes were serum-starved in Dulbecco's modified Eagle's medium containing 25 mM glucose for 16 h at 37 °C.

RESULTS

Absence of Adiponectin Had No Effect on Rimonabant-induced Suppression of Body Weight and Daily Food Intake—The body weight gain was similar between the untreated ob/ob and *adipo*(−/−)ob/ob mice (Fig. 1*A*), as reported previously (30). The food intake was also comparable between the untreated ob/ob and *adipo*(−/−)ob/ob mice (Fig. 1*B*). Rimonabant significantly decreased the body weight and food intake to similar degrees in the ob/ob and *adipo*(−/−)ob/ob mice (Fig. 1, *A* and *B*). After 21 days of rimonabant treatment, both the ob/ob and *adipo*(−/−)ob/ob mice weighed 10% less than the corresponding untreated mice (Fig. 1*A*). Moreover, rimonabant treatment significantly decreased the white adipose tissue (WAT) mass in both subcutaneous and visceral (epididymal, mesenteric, and retroperitoneal) fat to similar degrees in the ob/ob and *adipo*(−/−)ob/ob mice (Fig. 1*C*). To determine whether the presence of adiponectin is required for the reduction of the average adipocyte size induced by rimonabant treatment, we histologically analyzed the epididymal fat pad and subcutaneous WAT after fixation and quantitation of the adipocyte size. The distribution of the adipocyte size in the rimonabant-treated ob/ob and *adipo*(−/−)ob/ob mice was similarly narrowed to that in the untreated ob/ob and *adipo*(−/−)ob/ob mice (Fig. 1, *D* and *E*), and rimonabant treatment significantly reduced the average adipocyte size in the ob/ob and *adipo*(−/−)ob/ob mice to a similar degree (Fig. 1*F*). These findings indicate that the absence of adiponectin had no effect on either the rimonabant-induced decrease of the body weight or the food intake of the mice and that rimonabant treatment can induce a reduction of adipocyte size in the absence of adiponectin or leptin or both.

Rimonabant Increased the Energy Expenditure and Decreased the Serum Triglyceride and Free Fatty Acid Levels to a Similar Degree in the ob/ob and adipo(−/−)ob/ob Mice—In addition to suppressing food intake, rimonabant has been demonstrated to increase the energy expenditure (10, 34), and the increase in energy expenditure has also been shown in CB-1 receptor knock-out mice (35). Since the involvement of adiponectin in this action of rimonabant remains unclear, we investigated the effects of rimonabant on energy expenditure.

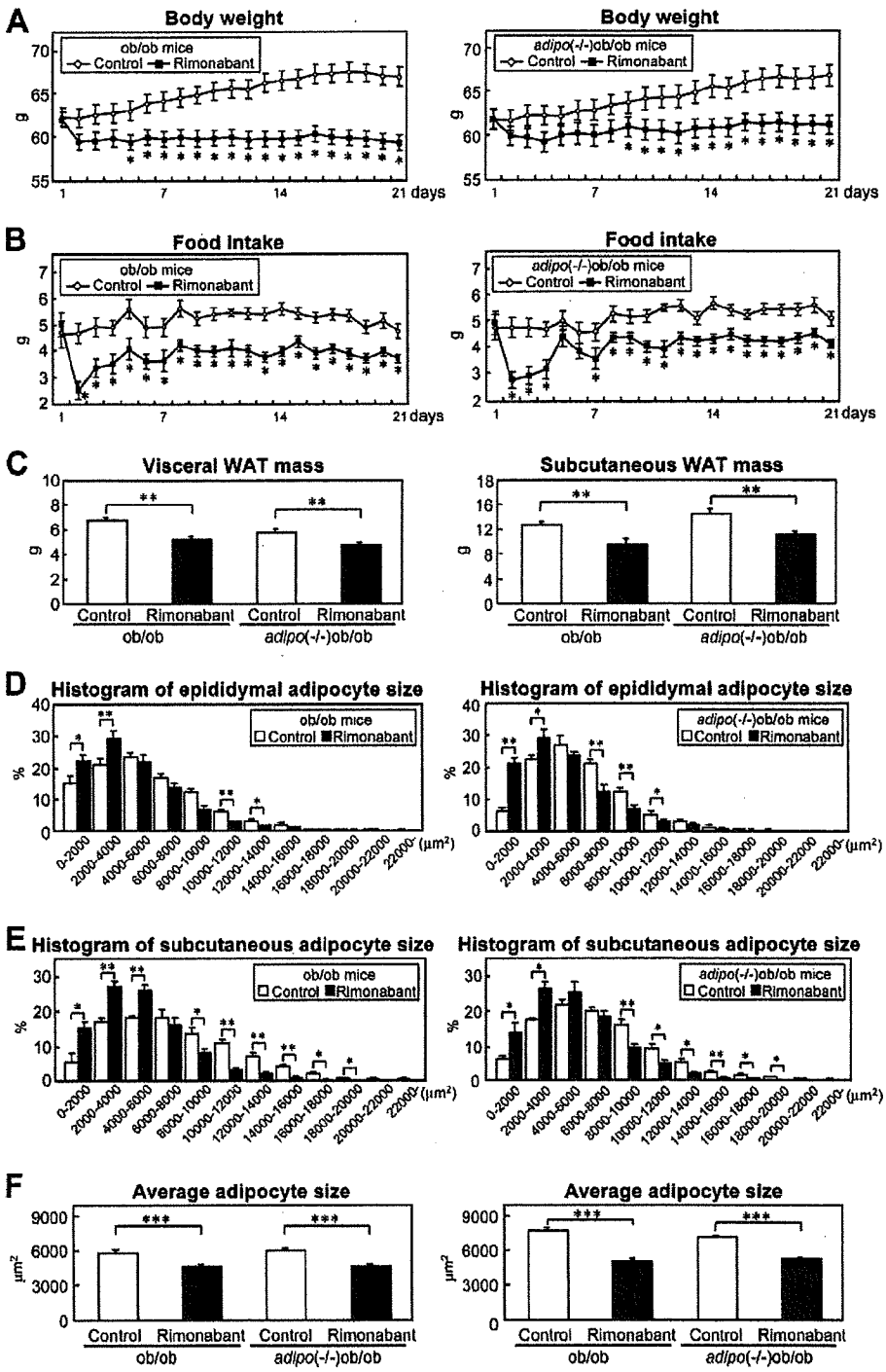

FIGURE 1. **The absence of adiponectin had no effect on rimonabant-induced suppression of body weight and daily food intake.** *A* and *B*, body weights (*A*) and food intake (*B*) of ob/ob (*left panels*) and *adipo*(−/−)ob/ob mice (*right panels*) not treated (*open squares*) and treated (*filled squares*) with rimonabant (n = 12–14/group). Values are means ± S.E. of data obtained from the analysis of ob/ob and *adipo*(−/−)ob/ob mice. *, $p < 0.05$. **, $p < 0.01$. *C*, weight of the total visceral white adipose tissue (*left panel*) and subcutaneous WAT (*right panel*) of ob/ob and *adipo*(−/−)ob/ob mice not treated (*open bars*) and treated (*filled bars*) with rimonabant (n = 9–14/group). Values are means ± S.E. of data obtained from the analysis of ob/ob and *adipo*(−/−)ob/ob mice. **, $p < 0.01$. *D* and *E*, histogram of adipocyte size from epididymal WAT (*D*) and subcutaneous WAT (*E*) of ob/ob (*left panels*) and *adipo*(−/−)ob/ob mice (*right panels*) not treated (*open bars*) and treated (*filled bars*) with rimonabant (n = 5–8/group). Values are means ± S.E. of data obtained from the analysis of ob/ob and *adipo*(−/−)ob/ob mice. *, $p < 0.05$; **, $p < 0.01$. *F*, average size of adipocyte from epididymal WAT (*left panel*) and subcutaneous WAT (*right panel*) of ob/ob and *adipo*(−/−)ob/ob mice not treated (*open bars*) and treated (*filled bars*) with rimonabant (n = 5–8/group). Values are means ± S.E. of data obtained from the analysis of ob/ob and *adipo*(−/−)ob/ob mice. ***, $p < 0.005$.

First, we measured the rectal temperature in the ob/ob and *adipo*(−/−)-ob/ob mice. The temperature was essentially the same (Fig. 2*A*), and rimonabant treatment significantly increased the rectal temperature of the ob/ob and *adipo*(−/−)ob/ob mice to a similar degree (Fig. 2*A*). Second, we investigated the oxygen consumption after 21-day treatment with rimonabant and found that in the dark phase of the daily light cycle, rimonabant increased the energy expenditure to a similar degree in both the ob/ob and *adipo*(−/−)-ob/ob mice (Fig. 2*B*). This effect of rimonabant on the energy expenditure in the ob/ob mice did not require the presence of adiponectin. We next investigated the effects of rimonabant treatment on the serum lipid levels. In addition to reducing the body weight, rimonabant has been demonstrated to reduce the serum triglyceride (TG) (15–18, 32) and free fatty acid (FFA) levels (32). However, the involvement of adiponectin in this action of rimonabant remains unclear. Both the serum TG and FFA levels were indistinguishable between the ob/ob and *adipo*(−/−)ob/ob mice (Fig. 2, *C* and *D*), and rimonabant treatment significantly decreased the levels of both to similar degrees in the ob/ob and *adipo*(−/−)ob/ob mice (Fig. 2, *C* and *D*). This effect of rimonabant on the serum lipids in the ob/ob mice did not require the presence of adiponectin. MCP-1 and resistin have been shown to be important mediators of insulin resistance linked to obesity (36–39). We analyzed the expression of MCP-1 and resistin in the epididymal WAT. The expressions of both MCP-1 and resistin were indistinguishable between the untreated and rimonabant-treated mice of either genotype (Fig. 2, *E* and *F*).

Rimonabant Increased the Plasma Adiponectin Levels in the ob/ob Mice, in Particular of High Molecular Weight Adiponectin—Rimonabant treatment for 21 days significantly increased the plasma adiponectin levels in the ob/ob mice, whereas plasma adiponectin was not detect-

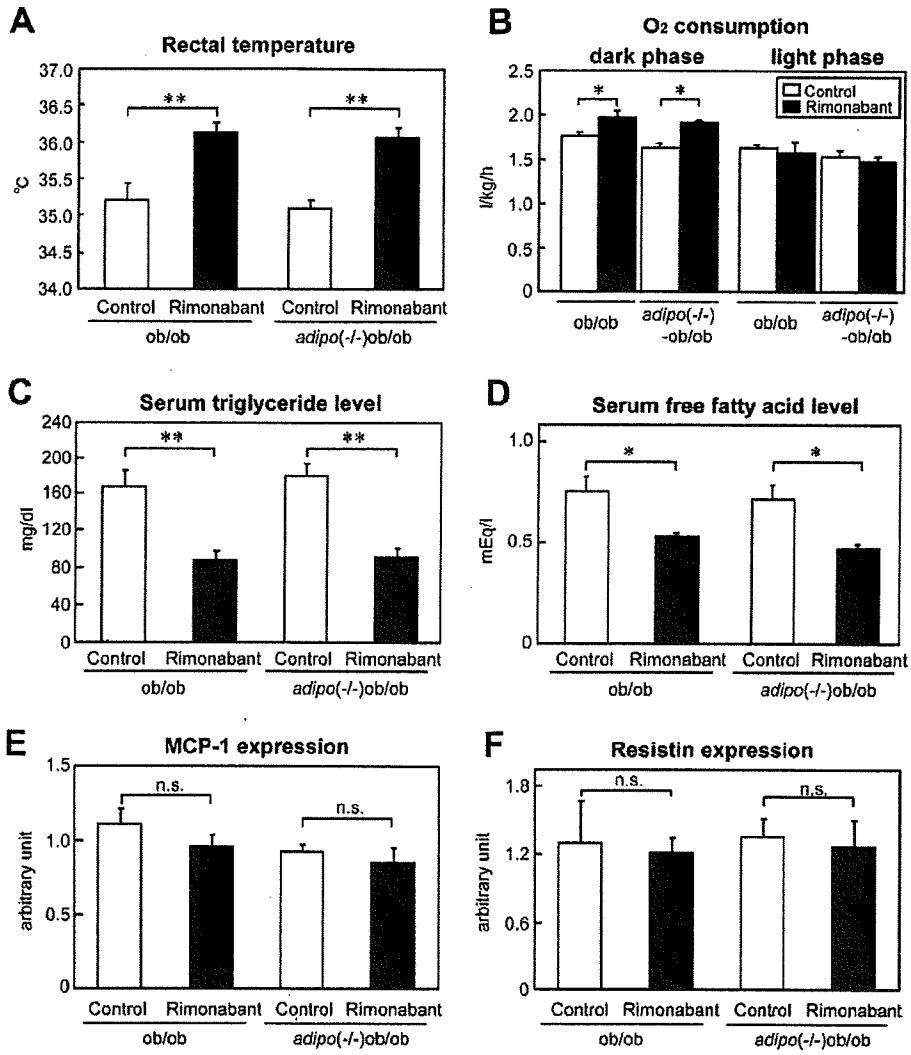

FIGURE 2. **Rimonabant increased the energy expenditure and decreased the serum triglyceride and free fatty acid levels to a similar degree in the ob/ob and *adipo*(−/−)ob/ob mice.** *A* and *B*, rectal temperature (*A*) and O_2 consumption (*B*) in ob/ob and *adipo*(−/−)ob/ob mice not treated (*open bars*) and treated (*filled bars*) with rimonabant (n = 6–10/group). Values are means ± S.E. of data obtained from the analysis of ob/ob mice and *adipo*(−/−)ob/ob mice. *, $p < 0.05$; **, $p < 0.01$. *C* and *D*, serum TG (*C*) and free fatty acid (*FFA*) (*D*) levels in ob/ob and *adipo*(−/−)ob/ob mice not treated (*open bars*) and treated (*filled bars*) with rimonabant. *C*, n = 11–14/group; *D*, n = 4–5/group. Values are means ± S.E. of data obtained from the analysis of ob/ob mice and *adipo*(−/−)ob/ob mice. *, $p < 0.05$. **, $p < 0.01$. *E* and *F*, MCP-1 (*E*) and resistin (*F*) expression levels in the epididymal WAT of ob/ob and *adipo*(−/−)ob/ob mice not treated (*open bars*) and treated (*filled bars*) with rimonabant (n = 7–8/group). Values are means ± S.E. of data obtained from the analysis of ob/ob mice and *adipo*(−/−)ob/ob mice. Values are means ± S.E. *n.s.*, not significant.

able in either the untreated or rimonabant-treated *adipo*(−/−)-ob/ob mice (Fig. 3*A*). High molecular weight (HMW) adiponectin is known to be the most active, and its serum levels have been reported to be decreased in obese individuals and murine models, which is associated with a decrease of the hepatic and muscle AMPK activity and fatty acid combustion and, thereby, exacerbation of insulin resistance (19, 20). Therefore, we analyzed the plasma levels of this isoform of adiponectin by Western blotting. Rimonabant treatment significantly increased the serum levels of HMW adiponectin in the ob/ob mice (Fig. 3*B*). On the other hand, the plasma levels of middle molecular weight and low molecular weight adiponectin were slightly, but not significantly, increased in the rimonabant-treated ob/ob mice (Fig. 3*B*). In regard to the *adipo*(−/−)-ob/ob mice, plasma adiponectin was not detectable in either the untreated or rimonabant-treated mice (Fig. 3*B*). Rimonabant has been reported to increase adiponectin expression and secretion in 3T3F442A adipocyte (6, 40). We next investigated the direct effect of rimonabant on adiponectin secretion using the murine adipocyte cell line 3T3L1 and confirmed that treatment with 100 nM and 1 μM rimonabant actually increased the expression and secretion into the medium of adiponectin (Fig. 3, *C* and *D*).

Rimonabant Improved Hepatic Insulin Resistance in both the ob/ob and adipo(−/−)ob/ob Mice, although the Effect Was Significantly Less Pronounced in the adipo(−/−)-ob/ob Mice—We carried out hyperinsulinemic-euglycemic clamp studies in the ob/ob and *adipo*(−/−)-ob/ob mice to investigate the effect of rimonabant on the insulin resistance in the liver and skeletal muscle. Without rimonabant treatment, the glucose infusion rates were comparable in the ob/ob and *adipo*(−/−)-ob/ob mice (Fig. 4*A*). After 21 days of rimonabant treatment, the glucose infusion rates were significantly increased in both the ob/ob and *adipo*(−/−)ob/ob mice (Fig. 4*A*); however, the increase was significantly less pronounced in the *adipo*(−/−)ob/ob mice. Rimonabant treatment also produced a significant decrease of the endogenous glucose production in both the ob/ob and *adipo*(−/−)ob/ob mice, but the effect was significantly less pronounced in the *adipo*(−/−)ob/ob mice (Fig. 4*B*). The rates of R_d were indistinguishable between the untreated ob/ob and *adipo*(−/−)ob/ob mice, and rimonabant treatment had no effect on this parameter in either genotype (Fig. 4*C*). We next studied the effects on insulin signaling and the downstream reactions in the liver (Fig. 4, *D* and *E*). Insulin-stimulated Akt phosphorylation was significantly increased in rimonabant-treated ob/ob mice as compared with that in the untreated ob/ob mice (Fig. 4*D*), whereas insulin-stimulated Akt phosphorylation only tended to be increased in the rimonabant-treated *adipo*(−/−)ob/ob mice as compared with that in the corresponding untreated mice. The PEPCK expression levels in the liver were comparable in the untreated ob/ob and

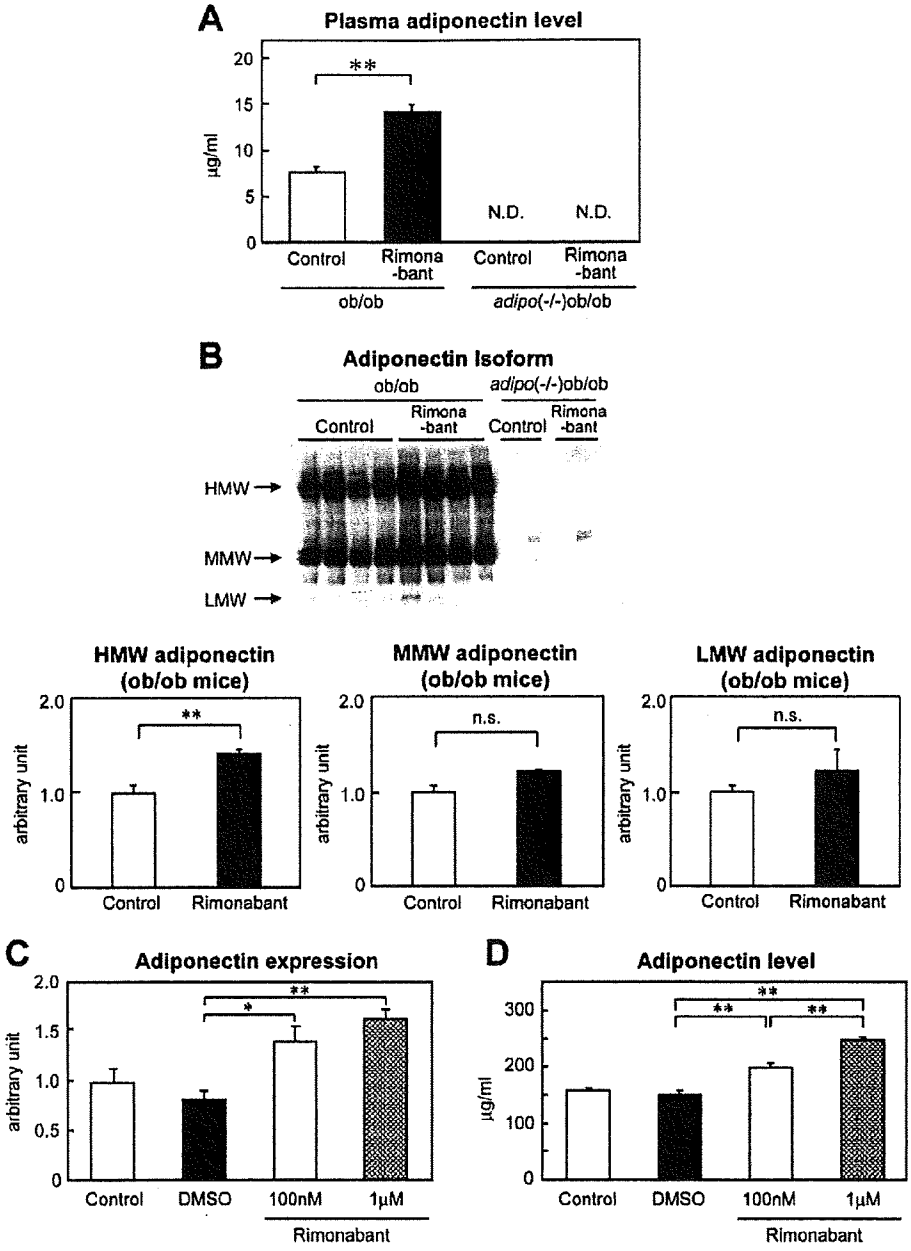

FIGURE 3. **Rimonabant increased the plasma adiponectin levels, in particular of high molecular weight adiponectin, in the ob/ob mice.** *A*, plasma adiponectin levels in ob/ob and *adipo*(−/−)ob/ob mice not treated (*open bar*) and treated (*filled bar*) with rimonabant (n = 7–14/group). Values are means ± S.E. of data obtained from the analysis of ob/ob mice and *adipo*(−/−)ob/ob mice. **, $p < 0.01$. *N.D.*, not detectable. *B*, the different isoforms of plasma adiponectin of ob/ob and *adipo*(−/−)ob/ob mice not treated (*open bars*) and treated (*filled bars*) with rimonabant were analyzed by Western blotting and quantitated by densitometry. The relative ratio of each molecular weight category of adiponectin was normalized to that in the control ob/ob mice not treated with rimonabant (n = 4–8/group). Results are representative of three independent experiments. Values are means ± S.E. of data obtained from the analysis of ob/ob mice and *adipo*(−/−)ob/ob mice. *, $p < 0.05$. *n.s.*, not significant. *C* and *D*, effects of rimonabant on adiponectin mRNA expression (*C*) and adiponectin secretion in the conditioned medium (*D*) of mouse 3T3L1 adipocytes (n = 4–9/group). Shown are controls (*open bars*), DMSO as the vehicle (*filled bars*), 100 nM rimonabant (*gray bars*), and 1 μM rimonabant (*latticed bars*). Values are means ± S.E. of data obtained from the analysis of 3T3L1 adipocytes. *, $p < 0.05$; **, $p < 0.01$.

adipo(−/−)ob/ob mice (Fig. 4*F*). Rimonabant treatment significantly decreased the expression of PEPCK in both the ob/ob and *adipo*(−/−)mice, but the effect was significantly less pronounced in the *adipo*(−/−)ob/ob mice (Fig. 4*F*). These findings indicate that rimonabant ameliorates hepatic but not muscle insulin resistance in mice with an ob/ob background, in both an adiponectin-dependent and adiponectin-independent manner.

Rimonabant Increased the Hepatic AMPK Activities and CPT-1 (Carnitine Palmitoyltransferase-1) Expression Levels in both ob/ob Mice and adipo(−/−)ob/ob Mice, but Its Effect was Significantly Less Pronounced in the adipo(−/−)-ob/ob Mice—We carried out analysis of the liver metabolic activity after the clamp studies to investigate the effect of rimonabant on amelioration of insulin resistance. The AMPK activities were comparable in the untreated ob/ob and *adipo*(−/−)ob/ob mice (Fig. 5*A*). Rimonabant treatment for 21 days increased the AMPK activities in both the ob/ob and *adipo*(−/−)-ob/ob mice, but its effect was significantly less pronounced in the *adipo*(−/−)ob/ob mice (Fig. 5*A*). The expression levels of CPT-1, the rate-limiting enzyme in fatty acid β-oxidation, were also comparable in the untreated ob/ob and *adipo*(−/−)ob/ob mice (Fig. 5*B*). Rimonabant treatment increased the CPT-1 expression in both ob/ob and *adipo*(−/−)ob/ob mice, but its effect was significantly less pronounced in the *adipo*(−/−)ob/ob mice (Fig. 5*B*). The expression levels of protein phosphatase 2C were indistinguishable between the untreated ob/ob and *adipo*(−/−)ob/ob mice, and rimonabant treatment had no effect on the protein phosphatase 2C expression in either genotype (Fig. 5*C*). As reported previously (26, 41), fatty acid oxidation is positively regulated by AMPK in the liver; therefore, we next carried out analysis of the hepatic TG content by Oil Red O staining. The percentage of areas of Oil Red O staining in the liver were comparable in the untreated ob/ob and *adipo*(−/−)ob/ob mice (Fig. 5*D*). Rimonabant treatment significantly decreased the hepatic TG content in both the ob/ob and *adipo*(−/−)mice, but its effect was significantly less pronounced in the *adipo*(−/−)ob/ob mice

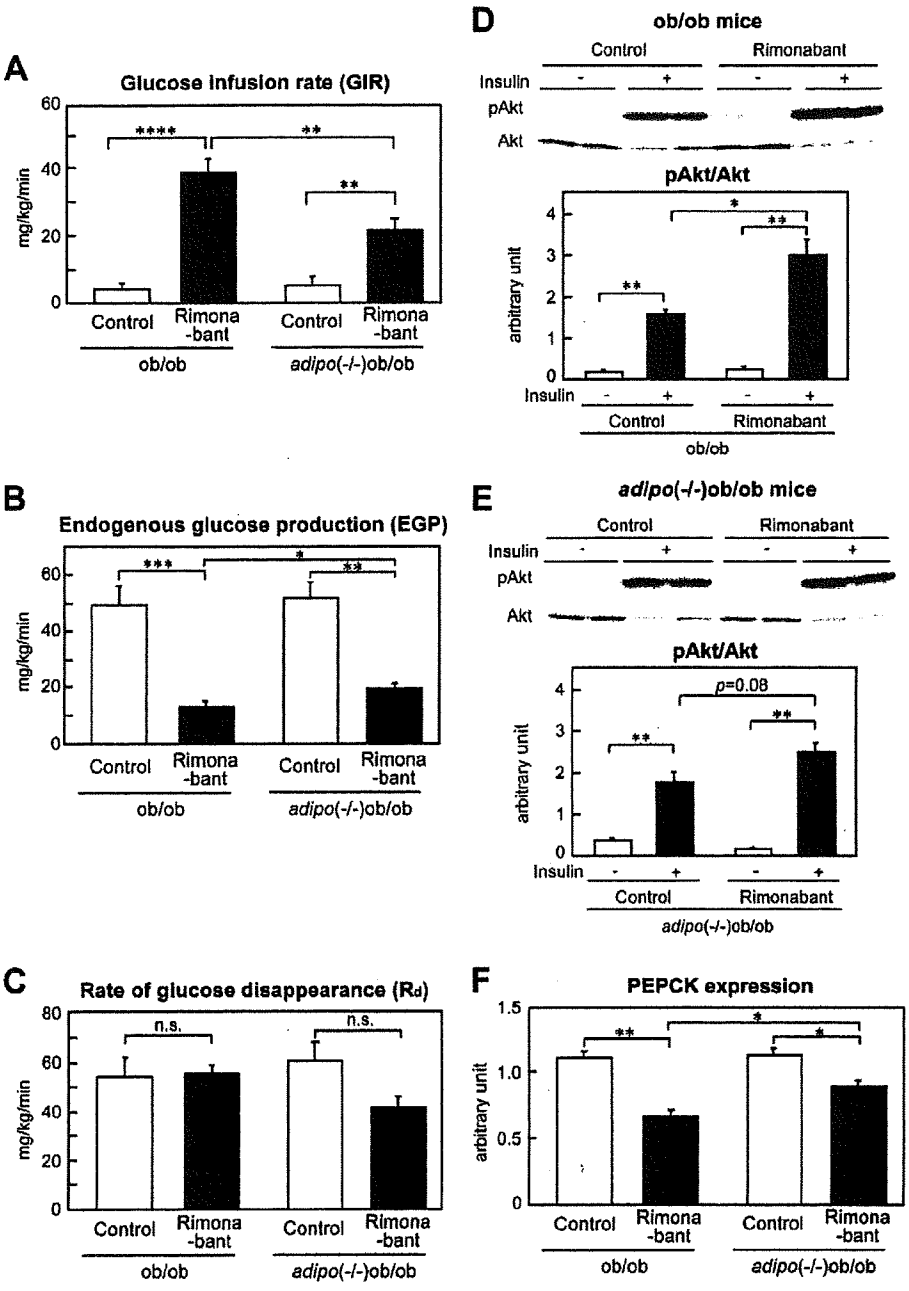

FIGURE 4. **Rimonabant improved hepatic insulin resistance in both ob/ob and *adipo*(−/−)ob/ob mice, although the effect was significantly less pronounced in the *adipo*(−/−)ob/ob mice.** *A–C*, glucose infusion rates (*GIR*) (*A*), endogenous glucose production (*EGP*) (*B*), and rates of glucose disappearance (*Rd*) (*C*) in ob/ob and *adipo*(−/−)ob/ob mice not treated (*open bars*) and treated (*filled bars*) with rimonabant in the clamp study (n = 5–7/group). Values are means ± S.E. of data obtained from the analysis of ob/ob mice and *adipo*(−/−)ob/ob mice. *, $p < 0.05$; **, $p < 0.01$; ***, $p < 0.005$. *D* and *E*, phosphorylations of Akt in the livers of ob/ob (*D*) and *adipo*(−/−)ob/ob mice (*E*) not treated (*open bars*) and treated (*filled bars*) with rimonabant after the injection of insulin (n = 4–5/group). Results are representative of three independent experiments. Values are means ± S.E. of data obtained from the analysis of ob/ob mice and *adipo*(−/−)ob/ob mice. *, $p < 0.05$. *F*, PEPCK expression levels in the livers of ob/ob and *adipo*(−/−)ob/ob mice not treated (*open bars*) and treated (*filled bars*) with rimonabant after the clamp studies (n = 6–7/group). The relative expressions after normalization to the expression level of cyclophilin were compared. Values are means ± S.E. of data obtained from the analysis of ob/ob mice and *adipo*(−/−)ob/ob mice. *, $p < 0.05$; **, $p < 0.01$. pAkt, phospho-Akt. *n.s.*, not significant.

(Fig. 5*D*). We also investigated the AMPK activities in the muscle after the clamp studies. The AMPK activities in the muscle were indistinguishable between the untreated ob/ob and *adipo*(−/−)ob/ob mice, and rimonabant treatment had no effect on the muscle AMPK activity in either genotype (Fig. 5*E*). These findings indicate that rimonabant activates hepatic but not muscle AMPK in mice with an ob/ob background in both an adiponectin-dependent and adiponectin-independent manner.

DISCUSSION

The selective CB-1 blocker rimonabant has been reported to produce weight loss and ameliorate insulin resistance and metabolic abnormalities in obese animals (12, 13), as also in patients with obesity (15–18). Rimonabant has also been reported to increase the plasma adiponectin levels in animal models of obesity and diabetes, as also in diabetic or nondiabetic subjects (15, 31, 32). Adiponectin has been proposed to be a major insulin-sensitizing adipokine (19, 20) and is a plausible candidate as the adipokine mediating the rimonabant-induced amelioration of insulin resistance. Therefore, in this study, we used two obesity models, the ob/ob and *adipo*(−/−)ob/ob mice, to investigate whether the rimonabant-induced increase of plasma adiponectin might be causally involved in the insulin-sensitizing effects of the drug.

Rimonabant treatment decreased the body weight, food intake, and weight of the WAT to similar degrees in the ob/ob and *adipo*(−/−)ob/ob mice. Furthermore, it also increased the energy expenditure and decreased the serum TG and FFA to similar degrees in the ob/ob and *adipo*(−/−)ob/ob mice. Thus, the involvement of adiponectin was not requited for rimonabant to exert its effects.

Significant improvement of the insulin resistance was observed in the ob/ob mice following rimonabant treatment, in association with significant up-regulation of the plasma adiponectin levels, in particular of HMW. Amelioration of insulin resistance in the ob/ob mice was considered to be attributable to improvement of the hepatic but not muscle insulin resistance. Interestingly, these

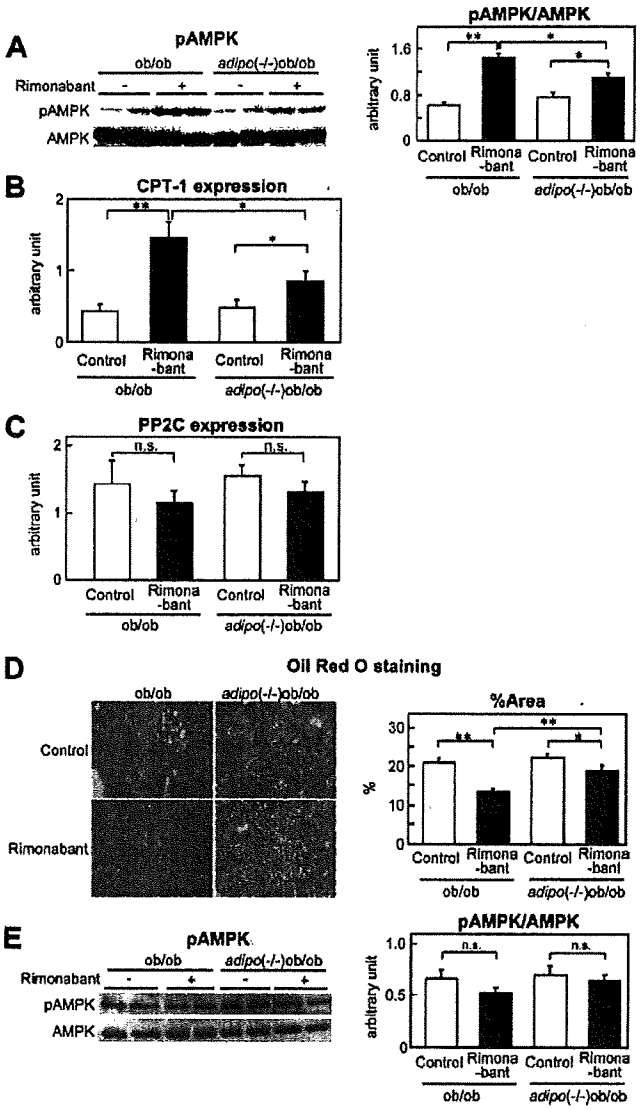

FIGURE 5. **Rimonabant increased the hepatic AMPK activities and CPT-1 expression levels in both ob/ob mice and *adipo*(−/−)ob/ob mice, but the effects were significantly less pronounced in the *adipo*(−/−)ob/ob mice.** *A*, phosphorylations of AMPK in the livers of ob/ob and *adipo*(−/−)ob/ob mice not treated (*open bars*) and treated (*filled bars*) with rimonabant after the clamp studies ($n = 4–5$/group). Results are representative of three independent experiments. Values are means ± S.E. of data obtained from the analysis of ob/ob mice and *adipo*(−/−)ob/ob mice. *, $p < 0.05$; **, $p < 0.01$. *B* and *C*, carnitine palmitoyltransferase-1 (*CPT-1*) (B) and protein phosphatase 2C (*PP2C*) (C) expression levels in the liver of ob/ob and *adipo*(−/−)ob/ob mice not treated (*open bars*) and treated (*filled bars*) with rimonabant after the clamp studies ($n = 4–9$/group). Relative expressions after normalization to the expression level of cyclophilin were compared. Values are means ± S.E. of data obtained from the analysis of ob/ob mice and *adipo*(−/−)ob/ob mice. *, $p < 0.05$; **, $p < 0.01$. *D*, Oil Red O staining in the livers of ob/ob and *adipo*(−/−)ob/ob mice not treated (*open bars*) and treated (*filled bars*) with rimonabant ($n = 6–10$/group). Representative liver histology as viewed on a computer monitor is shown. Original magnification, ×100. Values are means ± S.E. of data obtained from the analysis of ob/ob mice and *adipo*(−/−)ob/ob mice. *, $p < 0.05$; **, $p < 0.01$. *E*, phosphorylation levels of AMPK in the muscle of ob/ob and *adipo*(−/−)ob/ob mice not treated (*open bars*) and treated (*filled bars*) with rimonabant after the clamp studies ($n = 5$/group). Results are representative of three independent experiments. Values are means ± S.E. pAMPK, phospho-AMPK; *n.s.*, not significant.

improvements induced by rimonabant were significantly less pronounced in the *adipo*(−/−)ob/ob mice, indicating that adiponectin is involved in the rimonabant-mediated amelioration of hepatic insulin resistance. In fact, although a significant decrease of the PEPCK expression levels was observed, the AMPK activity was significantly increased, and the hepatic TG content was decreased in the ob/ob mice; all of these changes were significantly less pronounced in the *adipo*(−/−)ob/ob mice lacking adiponectin. We reported from a previous study that adiponectin, especially HMW adiponectin, stimulates AMPK activation in the liver (26, 42). These findings suggest that rimonabant treatment activates AMPK in the liver via increasing the secretion of HMW adiponectin and then decreases the expression of PEPCK to inhibit glucose production and increase CPT-1 expression, thereby stimulating fatty acid oxidation in the liver.

On the other hand, rimonabant treatment also produced significant amelioration of hepatic insulin resistance in the absence of adiponectin. This amelioration was possibly attributable to the reduction of body weight (Fig. 1*A*) but not to suppression of MCP-1 and resistin expression (Fig. 2, *E* and *F*). Alternatively, this amelioration was possibly due to the direct activation of AMPK by rimonabant in the liver. In fact, recent reports have shown that AMPK activity was significantly higher in the liver of hepatocyte-specific CB-1 receptor knock-out mice, although the serum adiponectin levels in these animals remained unchanged (35, 43), suggesting that rimonabant treatment directly activates hepatic AMPK, even without the mediation of adiponectin, and decreases the expression of PEPCK to inhibit glucose production in the liver.

In addition, Osei-Hyiaman *et al.* (35) have reported that CPT-1 activity in the liver was significantly increased when systemic CB-1 receptors were blocked pharmacologically in wild-type mice. Moreover, hepatic CPT-1 activity increased, and hepatic TG content decreased when hepatic CB-1 receptors were blocked genetically (35). These data suggest that CB-1 receptor blockade stimulates CPT-1 activity and increases fatty acid combustion to decrease the TG content in the liver. Consistent with this, rimonabant actually increased CPT-1 expression and decreased the TG content in the livers of ob/ob and *adipo*(−/−)ob/ob mice. However, these effects were markedly attenuated in the *adipo*(−/−)ob/ob mice, suggesting that increased CPT-1 expression and decreased hepatic TG content by rimonabant were also mediated by adiponectin-dependent as well as adiponectin-independent pathways.

Based on our findings, we propose that there are two distinct pathways by which rimonabant ameliorates insulin resistance, one an adiponectin-dependent pathway and the other an adiponectin-independent pathway (Fig. 6). Rimonabant increases the plasma levels of adiponectin, in particular of HMW adiponectin, which induces AMPK activation and decreases gluconeogenesis in the liver, thereby ameliorating insulin resistance. On the other hand, in a manner independent of adiponectin, rimonabant directly induces AMPK activation and decreases gluconeogenesis in the liver, possibly via the hepatic CB-1 receptor (35, 43), which also contributes to ameliorating insulin resistance. In addition, rimonabant decreases food intake and increases energy expenditure, which are related to reduction of body weight. This body weight loss may be also associated with ameliorating insulin resistance via adiponectin-dependent and adiponectin-independent pathways (Fig. 6).

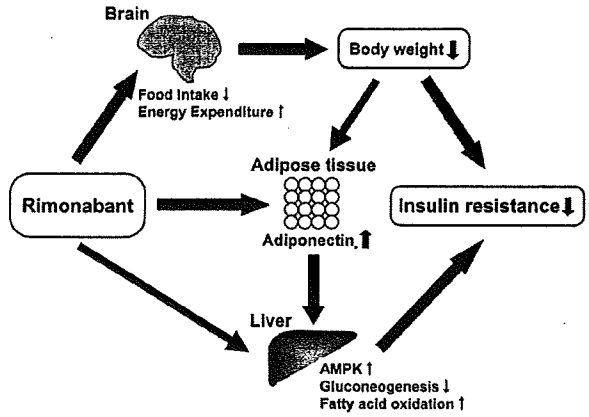

FIGURE 6. **Rimonabant ameliorates insulin resistance via both adiponectin-dependent and adiponectin-independent pathways.** There are two distinct pathways by which rimonabant ameliorates insulin resistance, one an adiponectin-dependent pathway and the other an adiponectin-independent pathway. Rimonabant increases the plasma levels of adiponectin, in particular of HMW adiponectin, which induces AMPK activation and decreases gluconeogenesis in the liver, thereby ameliorating insulin resistance. On the other hand, in a manner independent of adiponectin, rimonabant directly induces AMPK activation and decreases gluconeogenesis in the liver, possibly via hepatic CB-1 receptor, which also contributes to ameliorating insulin resistance. In addition, rimonabant decreases food intake and increases energy expenditure, which are related to reduction of body weight. This body weight loss may be also associated with ameliorating insulin resistance via adiponectin-dependent and adiponectin-independent pathways.

Rimonabant is metabolized in the liver by cytochrome P-450 CYP3A4 and amidohydrolase and excreted into the bile (44, 45). The oral bioavailability of rimonabant is low to moderate; this is due to the extensive first pass metabolism of the drug (European Medicines Agency). Therefore, in this study, the concentration in the liver of the orally administered rimonabant might be higher than that in other tissues, such as the muscle, because of the first pass effect of the liver. Although intraperitoneally administered rimonabant was reported in a previous study to significantly increase the glucose uptake in the soleus muscle of ob/ob mice (10), no improvement of the insulin resistance in the muscle was observed in our study. One of the reasons for this difference may be the lower concentration of rimonabant in the muscle due to the first pass effect of the liver.

In the four double-blind trials (RIO-Lipids (15), RIO-Europe (16), RIO-North America (17), and RIO-Diabetes (18)) the most frequent adverse events among individuals treated with rimonabant were nausea, dizziness, diarrhea, and insomnia, each occurring at a 1–9% greater frequency than that in the placebo group. In the RIO-Lipids, RIO-Europe, and RIO-North America, the drug had to be discontinued due to the development of psychiatric disorders (mainly depression) in 6–7% of rimonabant-treated individuals, an absolute increase of 2–5% over the frequency in the placebo group (44). Substance dependence with rimonabant has not been reported. The absence of the appearance of clinical signs in toxicology studies with a recovery period indicates that rimonabant does not possess the potential to produce withdrawal syndrome (European Medicines Agency).

Many reports have shown the efficacy of cannabinoid agonists in chronic pain (46). In a rodent model of inflammatory pain, anandamide, one of the endogenous cannabinoids, suppressed the development and maintenance of thermal hyperalgesia (47). This analgesic effect was diminished by concurrent administration of the CB-1 antagonist, rimonabant, and anandamide. Although rimonabant alters the sensitivity to pain (47), it does not necessarily induce pain itself. On the contrary, rimonabant has recently been shown to prevent indomethacin-induced intestinal injury by decreasing the levels of the proinflammatory cytokine, tumor necrosis factor α, in rodents (48), indicating its potential anti-inflammatory activity in acute and chronic diseases. In neurogenic inflammatory pain, including arthritis and neuropathy, many cytokines, especially tumor necrosis factor α, play a key role in the generation and maintenance of hyperalgesia (49). On the basis of these findings, Costa (50) indicated that the anti-tumor necrosis factor α effect of rimonabant might contribute to its anti-inflammatory activity and consequently to the relief of pain. However, further investigation and accumulation of further evidence on the effect of rimonabant on pain are needed. At least, in the four clinical trials mentioned above, side effects associated with pain, such as hyperalgesia or hypoalgesia, were not reported. Furthermore, it has been suggested that although females might perceive pain differently from males (51, 52), the anti-obesity effects of rimonabant appeared to be similar in males and females (European Medicines Agency).

In conclusion, this study demonstrated for the first time that rimonabant ameliorates insulin resistance via both adiponectin-dependent and adiponectin-independent pathways.

Acknowledgments—We thank Ritsuko Hoshino, Katsuyoshi Kumagai, Sayaka Sasamoto, Kayo Nishitani, Namiko Kasuga, and Hiroshi Chiyonobu for excellent technical assistance and animal care.

REFERENCES

1. Flier, J. S. (2004) *Cell* **116,** 337–350
2. Friedman, J. M. (2000) *Nature* **404,** 632–634
3. Reaven, G. M. (1988) *Diabetes* **37,** 1595–1607
4. Di Marzo, V., Goparaju, S. K., Wang, L., Liu, J., Bátkai, S., Járai, Z., Fezza, F., Miura, G. I., Palmiter, R. D., Sugiura, T., and Kunos, G. (2001) *Nature* **410,** 822–825
5. Cota, D., Marsicano, G., Tschöp, M., Grübler, Y., Flachskamm, C., Schubert, M., Auer, D., Yassouridis, A., Thöne-Reineke, C., Ortmann, S., Tomassoni, F., Cervino, C., Nisoli, E., Linthorst, A. C. E., Pasquali, R., Lutz, B., Stalla, G. K., and Pagotto, U. (2003) *J. Clin. Invest.* **112,** 423–431
6. Bensaid, M., Gary-Bobo, M., Esclangon, A., Maffrand, J. P., Le Fur, G., Oury-Donat, F., and Soubrié, P. (2003) *Mol. Pharmacol.* **63,** 908–914
7. Di Marzo, V., Bifulco, M., and De Petrocellis, L. (2004) *Nat. Rev. Drug Discov.* **3,** 771–784
8. Howlett, A. C., Breivogel, C. S., Childers, S. R., Deadwyler, S. A., Hampson, R. E., and Porrino, L. J. (2004) *Neuropharmacology* **47,** Suppl. 1, 345–358
9. Osei-Hyiaman, D., DePetrillo, M., Pacher, P., Liu, J., Radaeva, S., Bátkai, S., Harvey-White, J., Mackie, K., Offertáler, L., Wang, L., and Kunos, G. (2005) *J. Clin. Invest.* **115,** 1298–1305
10. Liu, Y. L., Connoley, I. P., Wilson, C. A., and Stock, M. J. (2005) *Int. J. Obes. Relat. Metab. Disord.* **29,** 183–187
11. Kola, B., Hubina, E., Tucci, S. A., Kirkham, T. C., Garcia, E. A., Mitchell, S. E., Williams, L. M., Hawley, S. A., Hardie, D. G., Grossman, A. B., and Korbonits, M. (2005) *J. Biol. Chem.* **280,** 25196–25201
12. Ravinet Trillou, C., Arnone, M., Delgorge, C., Gonalons, N., Keane, P., Maffrand, J. P., and Soubrié, P. (2003) *Am. J. Physiol.* **284,** R345–R353
13. Cota, D., Marsicano, G., Lutz, B., Vicennati, V., Stalla, G. K., Pasquali, R.,

and Pagotto, U. (2003) *Int. J. Obes. Relat. Metab. Disord.* **27,** 289–301
14. Matias, I., Gonthier, M. P., Orlando, P., Martiadis, V., De Petrocellis, L., Cervino, C., Petrosino, S., Hoareau, L, Festy, F., Pasquali, R., Roche, R., Maj, M., Pagotto, U., Monteleone, P., and Di Marzo, V. (2006) *J. Clin. Endocrinol. Metab.* **91,** 3171–3180
15. Després, J. P., Golay, A., and Sjöström, L. (2005) *N. Engl. J. Med.* **353,** 2121–2134
16. Van Gaal, L. F., Rissanen, A. M., Scheen, A. J., Ziegler, O., and Rössner, S. (2005) *Lancet* **365,** 1389–1397
17. Pi-Sunyer, F. X., Aronne, L. J., Heshmati, H. M., Devin, and Rosenstock, J. (2006) *J. Am. Med. Assoc.* **295,** 761–775
18. Scheen, A. J., Finer, N., Hollander, P., Jensen, M. D., and Van Gaal, L. F. (2006) *Lancet* **368,** 1660–1672
19. Kadowaki, T., Yamauchi, T., Kubota, N., Hara, K., Ueki, K., and Tobe, K. (2006) *J. Clin. Invest.* **116,** 1784–1792
20. Scherer, P. E. (2006) *Diabetes* **55,** 1537–1545
21. Yamauchi, T., Kamon, J., Waki, H., Terauchi, Y., Kubota, N., Hara, K., Mori, Y., Ide, T., Murakami, K., Tsuboyama-Kasaoka, N., Ezaki, O., Akanuma, Y., Gavrilova, O., Vinson, C., Reitman, M. L., Kagechika, H., Shudo, K., Yoda, M., Nakano, Y., Tobe, K., Nagai, R., Kimura, S., Tomita, M., Froguel, P., and Kadowaki, T. (2001) *Nat. Med.* **7,** 941–946
22. Berg, A. H., Combs, T. P., Du, X., Brownlee, M., and Scherer, P. E. (2001) *Nat. Med.* **7,** 947–953
23. Fruebis, J., Tsao, T. S., Javorschi, S., Ebbets-Reed, D., Erickson, M. R., Yen, F. T., Bihain, B. E., and Lodish, H. F. (2001) *Proc. Natl. Acad. Sci. U. S. A* **98,** 2005–2010
24. Kubota, N., Terauchi, Y., Yamauchi, T., Kubota, T., Moroi, M., Matsui, J., Eto, K., Yamashita, T., Kamon, J., Satoh, H., Yano, W., Froguel, P., Nagai, R., Kimura, S., Kadowaki, T., and Noda, T. (2002) *J. Biol. Chem.* **277,** 25863–25866
25. Nawrocki, A. R., Rajala, M. W., Tomas, E., Pajvani, U. B., Saha, A. K., Trumbauer, M. E., Pang, Z., Chen, A. S., Ruderman, N. B., Chen, H., Rossetti, L., and Scherer, P. E. (2006) *J. Biol. Chem.* **281,** 2654–2660
26. Yamauchi, T., Kamon, J., Minokoshi, Y., Ito, Y., Waki, H., Uchida, S., Yamashita, S., Noda, M., Kita, S., Ueki, K., Eto, K., Akanuma, Y., Froguel, P., Foufelle, F., Ferre, P., Carling, D., Kimura, S., Nagai, R., Kahn, B. B., and Kadowaki, T. (2002) *Nat. Med.* **8,** 1288–1295
27. Tomas, E., Tsao, T. S., Saha, A. K., Murrey, H. E., Zhang, Cc. C., Itani, S. I., Lodish, H. F., and Ruderman, N. B. (2002) *Proc. Natl. Acad. Sci. U. S. A* **99,** 16309–16313
28. Kemp, B. E., Stapleton, D., Campbell, D. J., Chen, Z. P., Murthy, S., Walter, M., Gupta, A., Adams, J. J., Katsis, F., van Denderen, B., Jennings, I. G., Iseli, T., Michell, B. J., and Witters, L. A. (2003) *Biochem. Soc. Trans.* **31,** 162–168
29. Hardie, D. G. (2004) *J. Cell Sci.* **117,** 5479–5487
30. Kubota, N., Terauchi, Y., Kubota, T., Kumagai, H., Itoh, S., Satoh, H., Yano, W., Ogata, H., Tokuyama, K., Takamoto, I., Mineyama, T., Ishikawa, M., Moroi, M., Sugi, S., Yamauchi, T., Ueki, K., Tobe, K., Noda, T., Nagai, R., and Kadowaki, T. (2006) *J. Biol. Chem.* **281,** 8748–8755
31. Poirier, B., Bidouard, J. P., Cadrouvele, C., Marniquet, X., Staels, B., O'Connor, S. E., Janiak, P., and Herbert, J. M. (2005) *Diabetes Obes. Metab.* **7,** 65–72
32. Gary-Bobo, M., Elachouri, G., Gallas, J. F., Janiak, P., Marini, P., Ravinet-Trillou, C., Chabbert, M., Cruccioli, N., Pfersdorff, C., Roque, C., Arnone, M, Croci, T., Soubrié, P., Oury-Donat, F., Maffrand, J. P., Scatton, B., Lacheretz, F., Le Fur, G., Herbert, J. M., and Bensaid, M. (2007) *Hepatology* **46,** 122–129
33. Kubota, N., Terauchi, Y., Miki, H., Tamemoto, H., Yamauchi, T., Komeda, K., Nakano, R., Ishii, C., Sugiyama, T., Eto, K., Tsubamoto, Y., Okuno, A., Murakami, K., Sekihara, H., Hasegawa, G., Naito, M., Toyoshima, Y., Tanaka, S., Shiota, K., Kitamura, T., Fujita, T., Ezaki, O., Aizawa, S., Nagai, R., Tobe, K., Kimura, S., and Kadowaki, T. (1999) *Mol. Cell* **4,** 597–609
34. Addy, C., Wright, H., Van Laere, K., Gantz, I., Erondu, N., Musser, B. J., Lu, K., Yuan, J., Sanabria-Bohórquez, S. M., Stoch, A., Stevens, C., Fong, T. M., De Lepeleire, I., Cilissen, C., Cote, J., Rosko, K., Gendrano, I. N., III, Nguyen, A. M., Gumbiner, B., Rothenberg, P., de Hoon, J., Bormans, G., Depré, M., Eng, W. S., Ravussin, E., Klein, S., Blundell, J., Herman, G. A., Burns, H. D., Hargreaves, R. J., Wagner, J., Gottesdiener, K., Amatruda, J. M., and Heymsfield, S. B. (2008) *Cell Metab.* **7,** 68–78
35. Osei-Hyiaman, D., Liu, J., Zhou, L., Godlewski, G., Harvey-White, J., Jeong, W., Batkai, S., Marsicano, G., Lutz, B., Buettner, C., and Kunos, G. (2008) *J. Clin. Invest.* **118,** 3160–3169
36. Kamei, N., Tobe, K., Suzuki, R., Ohsugi, M., Watanabe, T., Kubota, N., Ohtsuka-Kowatari, N., Kumagai, K., Sakamoto, K., Kobayashi, M., Yamauchi, T., Ueki, K., Oishi, Y., Nishimura, S., Manabe, I., Hashimoto, H., Ohnishi, Y., Ogata, H., Tokuyama, K., Tsunoda, M., Ide, T., Murakami, K., Nagai, R., and Kadowaki, T. (2006) *J. Biol. Chem.* **281,** 26602–26614
37. Steppan, C. M., Bailey, S. T., Bhat, S., Brown, E. J., Banerjee, R. R., Wright, C. M., Patel, H. R., Ahima, R. S., and Lazar, M. A. (2001) *Nature* **409,** 307–312
38. Kershaw, E. E., and Flier, J. S. (2004) *J. Clin. Endocrinol. Metab.* **89,** 2548–2556
39. Kanda, H., Tateya, S., Tamori, Y., Kotani, K., Hiasa, K., Kitazawa, R., Kitazawa, S., Miyachi, H., Maeda, S., Egashira, K., and Kasuga, M. (2006) *J. Clin. Invest.* **116,** 1494–1505
40. Gary-Bobo, M., Elachouri, G., Scatton, B., Le Fur, G., Oury-Donat, F., and Bensaid, M. (2006) *Mol. Pharmacol.* **69,** 471–478
41. Muoio, D. M., Seefeld, K., Witters, L. A., and Coleman, R. A. (1999) *Biochem. J.* **338,** 783–791
42. Hada, Y., Yamauchi, T., Waki, H., Tsuchida, A., Hara, K., Yago, H., Miyazaki, O., Ebinuma, H., and Kadowaki, T. (2007) *Biochem. Biophys. Res. Commun.* **356,** 487–493
43. Jeong, W., Osei-Hyiaman, D., Park, O., Liu, J., Bátkai, S., Mukhopadhyay, P., Horiguchi, N., Harvey-White, J., Marsicano, G., Lutz, B., Gao, B., and Kunos, G. (2008) *Cell Metab.* **7,** 227–235
44. Padwal, R. S., and Majumdar, S. R. (2007) *Lancet* **369,** 71–77
45. Xie, S., Furjanic, M. A., Ferrara, J. J., McAndrew, N. R., Ardino, E. L., Ngondara, A., Bernstein, Y., Thomas, K. J., Kim, E., Walker, J. M., Nagar, S., Ward, S. J., and Raffa, R. B. (2007) *J. Clin. Pharm. Ther.* **32,** 209–231
46. Hosking, R. D., and Zajicek, J. P. (2008) *Br. J. Anaesth.* **101,** 59–68
47. Richardson, J. D., Kilo, S., and Hargreaves, K. M. (1998) *Pain* **75,** 111–119
48. Croci, T., Landi, M., Galzin, A. M., and Marini, P. (2003) *Br. J. Phamacol.* **140,** 115–122
49. Schäfers, M., Geis, C., Svensson, C. I., Luo, Z. D., and Sommer, C. (2003) *Eur. J. Neurosci.* **17,** 791–804
50. Costa, B. (2007) *Br. J. Pharmacol.* **150,** 535–537
51. Hurley, R. W., and Adams, M. C. (2008) *Anesth. Analg.* **170,** 309–317
52. Chin, M. L., and Rosenquist, R. (2008) *Anesth. Analg.* **170,** 4–5

nature medicine

CD8$^+$ effector T cells contribute to macrophage recruitment and adipose tissue inflammation in obesity

Satoshi Nishimura[1–4], Ichiro Manabe[1,2,4,5], Mika Nagasaki[1,6], Koji Eto[7], Hiroshi Yamashita[1], Mitsuru Ohsugi[8], Makoto Otsu[7], Kazuo Hara[8], Kohjiro Ueki[3,5,8], Seiryo Sugiura[9], Kotaro Yoshimura[10], Takashi Kadowaki[3,5,8] & Ryozo Nagai[1,3,5]

Inflammation is increasingly regarded as a key process underlying metabolic diseases in obese individuals. In particular, obese adipose tissue shows features characteristic of active local inflammation. At present, however, little is known about the sequence of events that comprises the inflammatory cascade or the mechanism by which inflammation develops. We found that large numbers of CD8$^+$ effector T cells infiltrated obese epididymal adipose tissue in mice fed a high-fat diet, whereas the numbers of CD4$^+$ helper and regulatory T cells were diminished. The infiltration by CD8$^+$ T cells preceded the accumulation of macrophages, and immunological and genetic depletion of CD8$^+$ T cells lowered macrophage infiltration and adipose tissue inflammation and ameliorated systemic insulin resistance. Conversely, adoptive transfer of CD8$^+$ T cells to CD8-deficient mice aggravated adipose inflammation. Coculture and other *in vitro* experiments revealed a vicious cycle of interactions between CD8$^+$ T cells, macrophages and adipose tissue. Our findings suggest that obese adipose tissue activates CD8$^+$ T cells, which, in turn, promote the recruitment and activation of macrophages in this tissue. These results support the notion that CD8$^+$ T cells have an essential role in the initiation and propagation of adipose inflammation.

Inflammation is now considered to have a pivotal role in the development of metabolic diseases[1]. In particular, obese adipose tissue shows the hallmarks of chronic inflammation[2,3], and the inflammation is thought to alter adipose tissue function, leading to systemic insulin resistance[4]. The mechanism by which the development of this insulin resistance occurs is believed to involve proinflammatory cytokines produced by infiltrating macrophages and resident adipocytes within the obese adipose tissue[1]. Likewise, chronic inflammation also impairs triglyceride storage in adipose tissues, and the excess circulating free fatty acids and triglycerides also induces insulin resistance in muscle and liver[5–7]. Adding insult to injury, it has been postulated that a paracrine loop involving these free fatty acids and inflammatory cytokines establishes a vicious cycle that aggravates the inflammatory changes, furthering the dysfunction of adipose tissue[8]. As such, the inflammatory changes seen in obese adipose tissue may be the key pathology that promotes systemic inflammatory states and insulin resistance in obese individuals.

Macrophage infiltration of adipose tissue has been described in both mice and humans[1]. However, little is known about the sequence of events that lead to macrophage infiltration. Recently accumulation of other immune cells, such as T cells, has been documented in obese adipose tissue[9,10]. T lymphocytes are known to interact with macrophages and regulate the inflammatory cascade[11]. However, their functional role in adipose inflammation remains unclear. Here we show that infiltration of CD8$^+$ effector T cells is an early event during the development of adipose tissue obesity induced by a high-fat diet. Further, we show using loss- and gain-of-function approaches *in vivo* that these T cells are critical mediators of systemic metabolic dysfunction. Finally, we also show *in vitro* that obese adipose tissue can activate CD8$^+$ T cells, which, in turn, allows for the recruitment and differentiation of macrophages. Thus, together our findings indicate that CD8$^+$ T cells have essential roles in the initiation and maintenance of adipose tissue inflammation and systemic insulin resistance. Our results also clearly show the involvement of adaptive immunity in metabolic disorders.

RESULTS

CD8$^+$ T cell infiltration precedes macrophage accumulation

Adipose tissue consists of not only adipocytes but also stromal and vascular cells, including fibroblasts, vascular endothelial cells and inflammatory cells. This stromal vascular fraction is known to be essential for adipose tissue inflammation[2]. Therefore, to gain insight

[1]Department of Cardiovascular Medicine, [2]Nano-Bioengineering Education Program and [3]Translational Systems Biology and Medicine Initiative, Graduate School of Medicine, The University of Tokyo, Tokyo, Japan. [4]PRESTO, Japan Science and Technology Agency, Kawaguchi, Japan. [5]Comprehensive Center of Education and Research for Chemical Biology of the Diseases, [6]Computational Diagnostic Radiology and Preventive Medicine, The University of Tokyo, Tokyo, Japan. [7]Division of Stem Cell Therapy, Center for Stem Cell Biology and Regenerative Medicine, Institute of Medical Science, The University of Tokyo, Tokyo, Japan. [8]Department of Metabolic Diseases, Graduate School of Medicine, The University of Tokyo, Tokyo, Japan. [9]Department of Human and Engineered Environmental Studies, Graduate School of Frontier Sciences, The University of Tokyo, Tokyo, Japan. [10]Department of Plastic Surgery, Graduate School of Medicine, The University of Tokyo, Tokyo, Japan. Correspondence should be addressed to S.N. (snishi-tky@umin.ac.jp) or I.M. (manabe-tky@umin.ac.jp).

Received 5 January; accepted 7 April; published online 26 July 2009; doi:10.1038/nm.1964

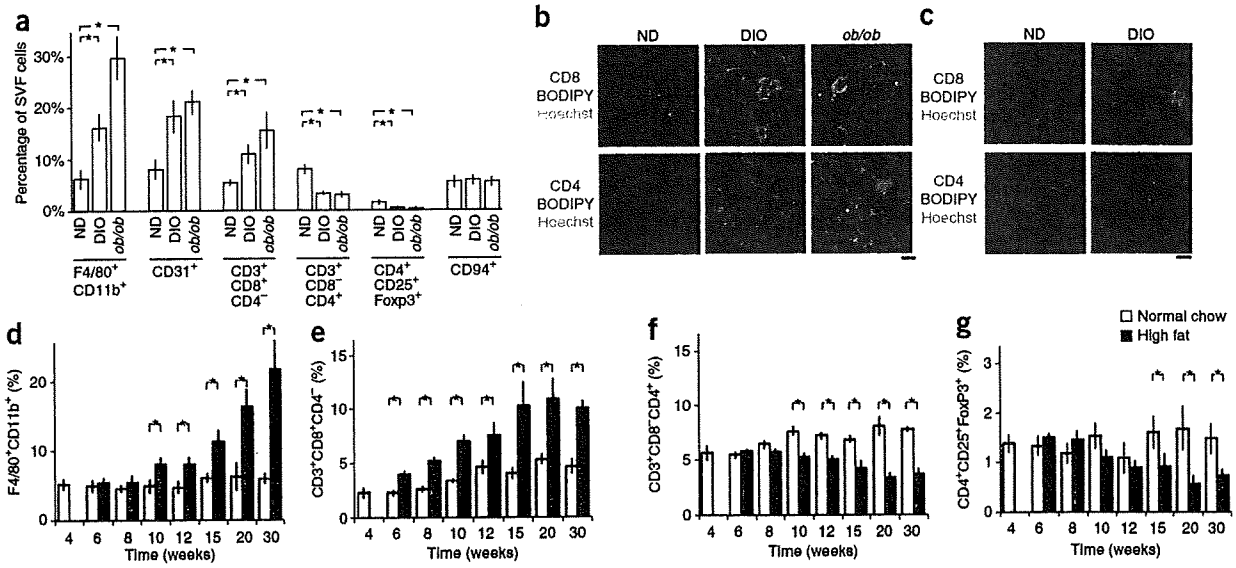

Figure 1 Differential infiltration of lymphocytes and macrophages into obese adipose tissue. (**a**) Flow cytometric analysis of the stromal vascular fraction (SVF) from the epididymal fat pads of control mice fed a normal chow diet (ND), diet-induced obese (DIO) mice fed a high-fat diet for 16 weeks and *ob/ob* mice fed a normal diet (*ob/ob*). All mice were 20-weeks-old. The cell populations of macrophages ($F4/80^+CD11b^+$), endothelial cells ($CD31^+$), $CD3^+CD8^+CD4^-$ T cells, $CD3^+CD8^-CD4^+$ T cells, regulatory T cells ($CD4^+CD25^+Foxp3^+$) and NK cells ($CD3^-CD94^+$) were analyzed ($n = 5$ mice in each group). The number of each cell type was normalized to the total number of viable SVF cells. $^*P < 0.05$. (**b**,**c**) Immunohistochemical analysis of CD8 and CD4 (each in red) in epididymal (**b**) and femoral subcutaneous (**c**) adipose tissue from ND, DIO and *ob/ob* mice. Adipocytes were counterstained with boron-dipyrromethene (BODIPY, blue) and nuclei with Hoechst (green). Quantification of $CD8^+$ and $CD4^+$ cells is shown in **Supplementary Fig. 3**. Scale bars, 100 μm. (**d**–**g**) Time courses of changes in the cell populations in the adipose stroma during development of obesity. Flow cytometric analysis of the stromal vascular fraction from the epididymal fat pads of control mice fed a normal chow diet and mice fed a high-fat diet beginning when they were 4-weeks-old. Numbers of macrophages (**d**), $CD8^+$ T cells (**e**), $CD4^+$ T cells (**f**) and regulatory T cells (**g**) were determined during the course of DIO development ($n = 5$ mice in each group; $^*P < 0.05$). Error bars represent means ± s.e.m.

into the inflammatory processes taking place within these cell fractions during obesity, we first analyzed immune cell populations in collagenase-digested stromal vascular fractions from obese epididymal adipose tissue with the aim of identifying local obesity-induced immunological changes. We acquired stromal vascular fractions using previously described methods of isolation[12] with a few modifications. We first carried out a set of flow cytometric analyses to determine the proper gating for analysis of lymphocytes and macrophages in adipose tissue (**Supplementary Fig. 1**). We found that R1 gating accounted for the majority of viable cells, including a majority of $F4/80^+CD11b^+$ macrophages. Because earlier studies used broader gating to analyze macrophages in the stromal vascular fraction[13], we compared the broader R2 gating with the narrower R1 gating. We found that the macrophage and lymphocyte fractions detected with R1 gating did not significantly differ from those detected using the broader R2 gating (**Supplementary Fig. 1** and **Supplementary Table 1**). For that reason, we analyzed subsequent cell fractions by R1 gating (for further discussion of gating, see **Supplementary Methods** and **Supplementary Fig. 1**).

Consistent with earlier reports[2], the infiltration of $F4/80^+CD11b^+$ macrophages into adipose tissue was significantly increased by diet-induced obesity (DIO) and in obese *ob/ob* mice compared to the control lean mice on a normal diet ($P < 0.05$) (**Fig. 1a**). The numbers of $CD31^+$ endothelial cells were also higher in obese mice (**Fig. 1a**), which may reflect angiogenesis[14]. Notably, we found that $CD3^+$ T cells accounted for 14.8 ± 0.9% of stromal vascular cells in lean adipose tissue, and most (94.7 ± 0.3%) of the $CD3^+$ T cells were CD4 or CD8 positive. The $CD3^+CD8^+CD4^-$ T cell fraction was larger in obese adipose tissue, whereas the $CD3^+CD4^+CD8^-$ T cell fraction was smaller, as was the regulatory T cell fraction ($CD4^+CD25^+Foxp3^+$) compared to lean mice on normal diet ($P < 0.05$). The natural killer (NK) cell fraction ($CD3^-CD94^+$) was unaffected by obesity (**Fig. 1a**). In contrast to the higher number of $CD8^+$ lymphocytes seen in obese adipose tissue, $CD8^+$ and $CD4^+$ T cell counts were significantly lower in peripheral blood from *ob/ob* mice and were unchanged in DIO mice as compared to mice on a normal diet ($P < 0.05$) (**Supplementary Fig. 2**), suggesting selective recruitment of $CD8^+$ T lymphocytes to obese adipose tissues.

Immunohistochemical analysis of F4/80, CD8 and CD4 expression also revealed higher numbers of $F4/80^+$ macrophages and $CD8^+$ T cells and lower numbers of $CD4^+$ T cells in obese epididymal fat pads as compared to mice on a normal diet ($P < 0.05$) (**Fig. 1b** and **Supplementary Fig. 3**). By contrast, we found no significant changes in the numbers of $CD8^+$ and $CD4^+$ cells in subcutaneous fat pads (**Fig. 1c**). In obese epididymal adipose tissues, we found a number of $CD8^+$ cells within 'crown-like structures' (CLSs), which reflect the focal convergence of macrophages surrounding necrotic adipocytes[14,15] (**Fig. 1b**), whereas $CD4^+$ cells showed no apparent relationship with CLSs.

Most $CD3^+CD8^+$ cells were $CD62L^-$ and $CD44^+$ (74.7% ± 3.8% of $CD3^+$ $CD8^+$ cells in DIO mice), suggesting the majority of infiltrated $CD8^+$ T cells were activated effector T cells[16]. To assess the clonality of $CD8^+$ in obese adipose, we examined the T cell receptor (TCR) V_β repertoire of $CD8^+$ T cells in lean and obese adipose tissues. The results showed that $CD8^+$ T cells in obese adipose were not monoclonal, though the $CD8^+$ cell fractions that were positive for $V_{\beta 7}$ and $V_{\beta 20b}$ were significantly larger in obese adipose tissues as compared to mice on a normal diet ($P < 0.05$) (**Supplementary Fig. 4**).

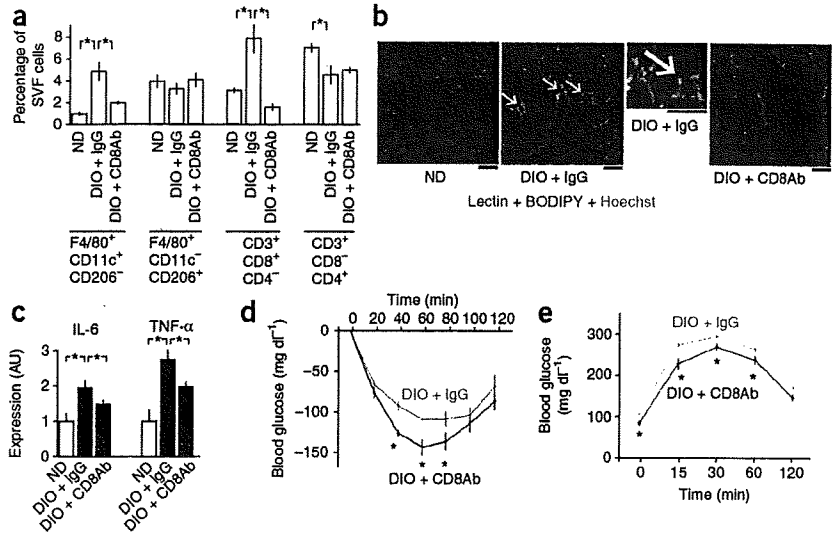

Figure 2 Effects of CD8-specific antibody treatment on obese adipose tissue inflammation. (**a**) Flow cytometric analysis of M1 macrophages ($F4/80^+CD11c^+CD206^-$), M2 macrophages ($F4/80^+CD11c^-CD206^+$), $CD8^+$ T cells and $CD4^+$ T cells in stromal vascular fractions in mice from lean normal-diet (ND), and DIO mice administered either antibody to CD8 (DIO + CD8Ab) or control IgG (DIO + IgG). The same mice were used in **b–e**. High-fat diet was started at the age of 4-weeks-old, and all of the mice were examined at 12-weeks-old. ($n = 5$ mice in each group). (**b**) Histochemical identification of endothelial cells (lectin, red), adipocytes (BODIPY, blue) and nuclei (Hoechst, green) in epididymal adipose tissue. White arrows indicate CLSs. Scale bars, 100 μm. (**c**) Real-time PCR analysis of cytokine expression in adipose tissue. The levels of each transcript were normalized to that in the lean control ($n = 5$ mice in each group). AU, arbitrary units. (**d,e**) Results of insulin tolerance (**d**, 0.75 U insulin per kg body weight) and oral glucose tolerance (**e**, 1 g per kg glucose) tests in DIO mice treated with antibody to CD8 or control IgG ($n = 8$ mice in each group). $^*P < 0.05$. Error bars represent means ± s.e.m.

It is known that one consequence of macrophage accumulation, particularly M1 macrophages, in inflamed adipose tissue is modulation and impairment of the tissue's function[17]. It is not known, however, what initiates macrophage infiltration or the resultant inflammatory cascade. The dynamic changes in lymphocyte populations seen in obese adipose tissue (**Fig. 1a,b**) suggest that lymphocytes might have a key role. To test this idea, we examined the time course of changes in stromal cell populations during the progression of DIO. We fed C57BL/6 mice a high-fat diet, beginning when they were 4-weeks-old (**Fig. 1d–g**). Within 2 weeks, the $CD8^+CD4^-$ T cell fraction within the total stromal vascular cell fraction was significantly increased in the stroma of the epididymal fat, as compared to that in mice fed a control chow diet (**Fig. 1e**). The numbers of $CD8^+CD4^-$ T cells continued to increase thereafter, peaking when the mice were 15-weeks-old (**Fig. 1e**). By contrast, the fractions of $CD8^-CD4^+$ T cells and $CD4^+CD25^+FoxP3^+$ regulatory T cells were reduced at later times (**Fig. 1f,g**), suggesting that $CD8^+$ T cell infiltration is a primary event during inflammatory cascades within adipose tissue. The increase in $CD8^+$ T cells also preceded the accumulation of macrophages when cell numbers were expressed per fat pad (**Supplementary Fig. 5**), clearly indicating that $CD8^+$ cells infiltrated into the epididymal fat pads of DIO mice before macrophage infiltration.

To gain additional insight into the clinical importance of $CD8^+$ T cells in obese fat, we analyzed the expression of *CD8A* in samples of human subcutaneous adipose tissue. Levels of *CD8A* expression were significantly higher in obese subjects than in lean ones ($P < 0.05$), suggesting that $CD8^+$ T cells also accumulate in human obese adipose tissue (**Supplementary Fig. 6**).

CD8 depletion inhibits inflammatory cascade in obese adipose

To assess the role of $CD8^+$ T cells in adipose inflammation, we examined the effects of CD8 depletion using neutralizing antibody treatment on the inflammatory response in obese adipose tissue. We randomly assigned male C57BL/6 mice to two groups and intraperitoneally administered either antibody to CD8 or control IgG once a week for 8 weeks, beginning when the mice were 4-weeks-old. We fed the mice a high-fat diet over the same period, and we performed metabolic and histological analyses at 12 weeks of age. Antibody to CD8 treatment had no effect on body weight, food intake, fat pad weight or adipocyte diameter (**Supplementary Fig. 7**). However, it significantly lowered the $CD8^+CD4^-$ T cell fraction in the epididymal fat pads without affecting the $CD8^-CD4^+$ cell fraction (**Fig. 2a**). It also reduced the infiltrated M1 macrophage ($F4/80^+CD11c^+CD206^-$) fraction without affecting the M2 macrophage ($F4/80^+CD11c^-CD206^+$) fraction[17] and significantly lowered the numbers of CLSs ($P < 0.05$ for each) (**Fig. 2b** and **Supplementary Fig. 7d**).

The messenger RNA expression of the proinflammatory cytokines interleukin-6 (IL-6) and tumor necrosis factor-α (TNF-α) in epididymal fat pads was lowered by CD8-specific antibody treatment (**Fig. 2c**), as were their serum concentrations (**Supplementary Fig. 7f**). In addition, the insulin resistance and glucose intolerance induced by the high-fat diet were ameliorated by CD8-specific antibody treatment (**Fig. 2d,e**). Similarly, CD8-specific antibody treatment lowered M1 macrophage infiltration into epididymal fat and ameliorated systemic insulin resistance in *ob/ob* mice (**Supplementary Fig. 8**). Collectively, these effects of CD8-specific antibody treatment clearly show that $CD8^+$ cells are required for the recruitment of macrophages into obese adipose tissue and the initiation and propagation of inflammatory responses there.

CD8 depletion ameliorates pre-established inflammation

We next examined the activity of $CD8^+$ T cells in obese adipose tissues in which inflammation had already been established. We began administering antibodies to 19-week-old DIO mice that had been fed a high-fat diet since they were 9-weeks-old. We intraperitoneally administered either antibody to CD8 or control IgG three times per week for 2 weeks, and examined the mice at 21-weeks-old. Treatment with antibody to CD8 suppressed $CD8^+$ T cell infiltration into obese fat pads without affecting $CD4^+$ T cells (**Fig. 3a**). CD8 antibody also lowered M1 ($F4/80^+CD11c^+$) macrophage fraction while leaving the M2 macrophage ($F4/80^+CD11c^-$) fraction unchanged (**Fig. 3a**). The reduction in macrophage infiltration was confirmed by F4/80 immunohistochemistry (**Fig. 3b**). In addition, the number of CLSs was also lowered by CD8-specific antibody treatment (**Fig. 3b,c**). DIO led to upregulated mRNA expression of the proinflammatory cytokines IL-1, IL-6 and TNF-α, as well as of

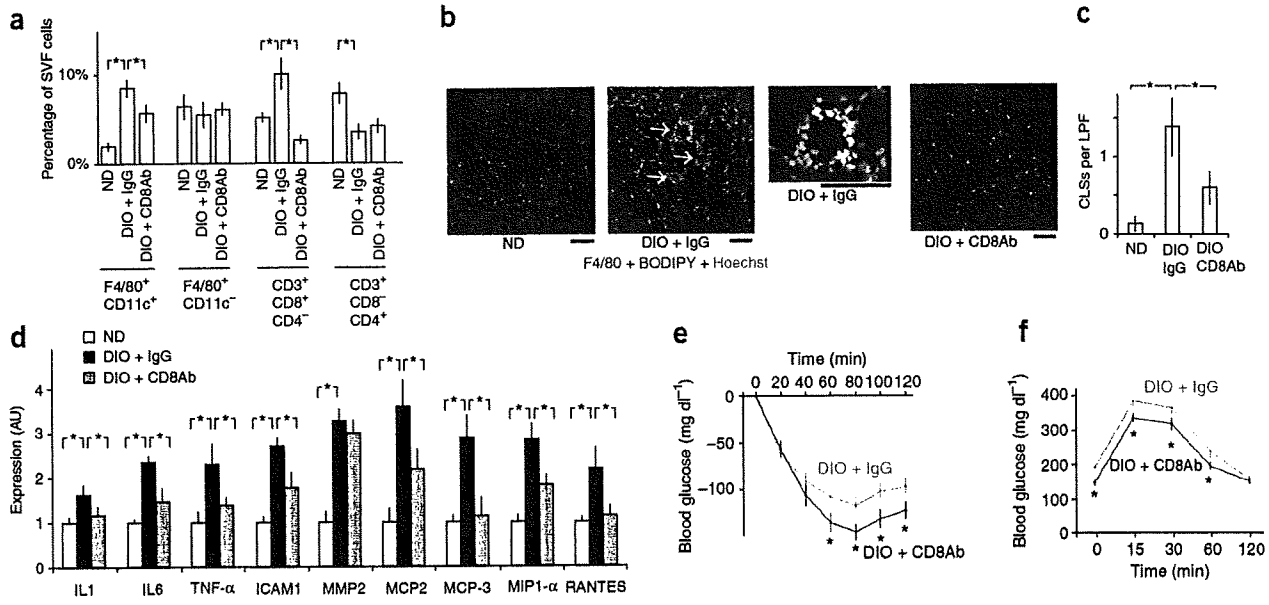

Figure 3 Effects of CD8-specific antibody treatment on pre-established obese adipose inflammation. **(a)** Flow cytometric analysis of cell populations in stromal vascular fractions from control mice on a normal chow diet (ND) and DIO mice administered control IgG (DIO + IgG) or antibody to CD8 (DIO + CD8Ab) three times per week from 19- to 21-weeks-old. ($n = 5$ mice in each group). High-fat diet was started at the age of 9-weeks-old, and all the mice were examined at 21-weeks-old. The same mice were used in **b–f**. **(b)** Immunohistochemical identification of macrophages (F4/80, red) in epididymal adipose tissue. Adipocytes were counterstained with BODIPY (blue), and the nuclei with Hoechst (green). Scale bars, 100 μm. **(c)** Numbers of CLSs (shown by white arrows in **b**) in adipose tissue ($n = 20$ low-power fields (LPF) in each group). **(d)** Real-time PCR analysis of cytokine expression in epididymal adipose tissue. The levels of each transcript were normalized to those in control ND mice. MIP, monocyte inflammatory protein ($n = 5$ mice in each group). **(e,f)** Results of insulin tolerance (**e**, 1 U insulin per kg body weight) and oral glucose tolerance (**f**, 1 g per kg glucose) tests in DIO mice treated with antibody to CD8 or control IgG ($n = 10$ mice in each group). $^*P < 0.05$. Error bars represent means ± s.e.m.

intercellular adhesion molecule-1 (ICAM1) and matrix metalloproteinase-2 (MMP-2), in adipose tissue, which is consistent with local inflammation, and CD8-specific antibody treatment lowered expression of all of these mediators (**Fig. 3d**).

CD8-specific antibody treatment also ameliorated insulin resistance and glucose intolerance in DIO mice (**Fig. 3e,f** and **Supplementary Fig. 9**). These results clearly show that CD8-specific antibody treatment suppresses preexisting adipose inflammation, which strongly suggests that $CD8^+$ cells are required for the maintenance of inflammatory reactions in obese adipose tissue.

$CD8^+$ T cells are required for adipose tissue inflammation

To further establish the requirement for $CD8^+$ T cells in adipose inflammation *in vivo*, we started 6-week-old genetically CD8-deficient mice on a high-fat diet and maintained them on it for 8 weeks, and examined the $CD8a^{-/-}$ mice at 14-weeks-old. In sharp contrast to wild-type mice fed the same high-fat diet (**Fig. 1**), the CD8-deficient mice did not show significant increases in the M1 or M2 macrophage fraction in the epididymal fat under high-fat diet (**Fig. 4a**), and we found very few CLSs (**Fig. 4b,c**), although both body weight and epididymal fat mass were significantly higher compared to $CD8a^{-/-}$ mice on a normal diet (**Supplementary Fig. 10a,b**). Levels of proinflammatory cytokine mRNA expression in adipose tissue, including IL-6 and TNF-α, also were not increased by the high-fat diet in CD8-deficient mice (**Fig. 4d**).

To directly examine the role of $CD8^+$ T cells in adipose tissue inflammation, we adoptively transferred splenic $CD8^+$ T cells into CD8-deficient mice. We intravenously administered either 5×10^6 splenic $CD8^+$ T cells isolated from 7-week-old C57BL/6 mice or control vehicle weekly over the same period and examined the $CD8a^{-/-}$ mice at 14-weeks-old. Adoptive transfer of $CD8^+$ T cells increased M1 macrophage infiltration (**Fig. 4a**), numbers of CLSs (**Fig. 4b,c**), and expression of IL-6 and TNF-α in epididymal fat (**Fig. 4d**), indicating initiation of adipose inflammation. A high-fat diet induced moderate glucose intolerance in untreated CD8-deficient mice, but we did not observe insulin resistance in insulin tolerance tests (**Fig. 4e,f**). Adoptive $CD8^+$ T cell transfer aggravated the glucose intolerance and induced insulin resistance (**Fig. 4e,f**). Taken together, the results that we obtained with CD8-deficient mice confirm that $CD8^+$ T cells are essential for macrophage recruitment and inflammation in adipose tissue in DIO.

Interplay between macrophages, T cells and adipocytes

We next analyzed the cellular interplay via which inflammation develops in obese adipose tissue. On the basis of the findings of the *in vivo* experiments summarized above, we hypothesized that obese adipose tissue activates $CD8^+$ T cells, which, in turn, recruit and activate macrophages. To test this hypothesis, we first cocultured splenic $CD8^+$ T cells with epididymal fat tissue prepared from lean or obese mice to determine whether obese adipose tissue can activate $CD8^+$ T cells. Whereas obese epididymal fat clearly induced T cell proliferation, lean fat did so only modestly (**Fig. 5a**), indicating that obese adipose tissue can indeed activate $CD8^+$ T cells.

To assess the involvement of $CD8^+$ T cells in monocytes and macrophage differentiation, we cocultured various combinations of peripheral blood $CD11b^{high}$ granulocyte-1 $(Gr\text{-}1)^-CD4^-CD8^-$cells (most of which were monocytes), $CD8^+$ cells prepared from either lean or obese adipose tissue, and lean epididymal adipose tissue. By

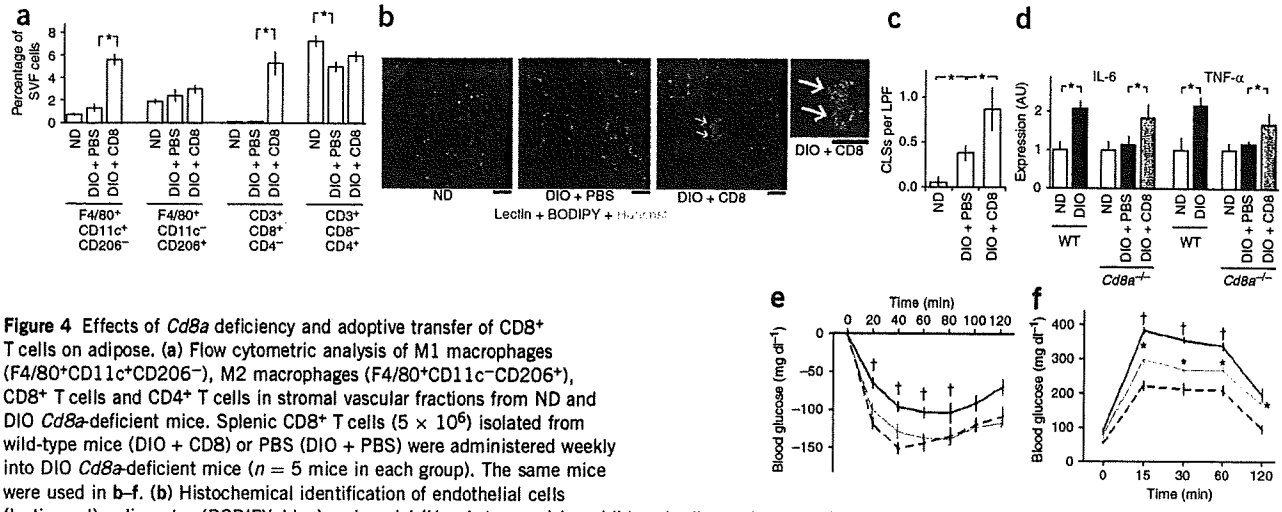

Figure 4 Effects of *Cd8a* deficiency and adoptive transfer of CD8+ T cells on adipose. (**a**) Flow cytometric analysis of M1 macrophages ($F4/80^+CD11c^+CD206^-$), M2 macrophages ($F4/80^+CD11c^-CD206^+$), $CD8^+$ T cells and $CD4^+$ T cells in stromal vascular fractions from ND and DIO *Cd8a*-deficient mice. Splenic $CD8^+$ T cells (5×10^6) isolated from wild-type mice (DIO + CD8) or PBS (DIO + PBS) were administered weekly into DIO *Cd8a*-deficient mice ($n = 5$ mice in each group). The same mice were used in **b–f**. (**b**) Histochemical identification of endothelial cells (lectin, red), adipocytes (BODIPY, blue) and nuclei (Hoechst, green) in epididymal adipose tissue. White arrows indicate CLSs. Scale bars, 100 μm. (**c**) Numbers of CLSs in adipose tissues ($n = 20$ low-power fields in each group). (**d**) Real-time PCR analysis of cytokine expression in adipose tissue from C57BL/6 (WT) ND, WT DIO, and *Cd8a*-deficient ND, DIO + CD8 or DIO + PBS mice. ($n = 5$ mice in each group). $^*P < 0.05$ in **a–d**. (**e,f**) Insulin tolerance (**e**, 0.75 U insulin per kg body weight) and oral glucose tolerance (**f**, 1 g per kg) tests of the *Cd8a*-deficient ND (dotted lines), DIO + CD8 and DIO + PBS groups ($n = 6$ mice in each group). $^*P < 0.05$ for ND versus DIO + PBS and $\dagger P < 0.05$ for DIO + PBS versus DIO + CD8. Error bars represent means ± s.e.m.

themselves, neither $CD8^+$ cells nor adipose tissue induced macrophage differentiation (**Fig. 5b**). However, when cocultured with both $CD8^+$ cells and lean adipose tissue, peripheral blood monocytes differentiated into $F4/80^+CD11b^+CD68^+$ macrophages (**Fig. 5b**). Moreover, $CD8^+$ cells from obese adipose tissues generated significantly more macrophages than those from lean adipose (**Fig. 5b**). Thus, $CD8^+$ cells seem to be essential for macrophage differentiation in this setting. Further, the requirement for adipose tissue suggests that the interaction between $CD8^+$ T cells and adipose tissue is necessary for induction of macrophage differentiation.

We then tested whether activated $CD8^+$ cells elicit macrophage migration via humoral interactions. Analysis of the medium conditioned with activated $CD8^+$ T cells showed that these cells secrete substantial amounts of humoral factors known to induce macrophage

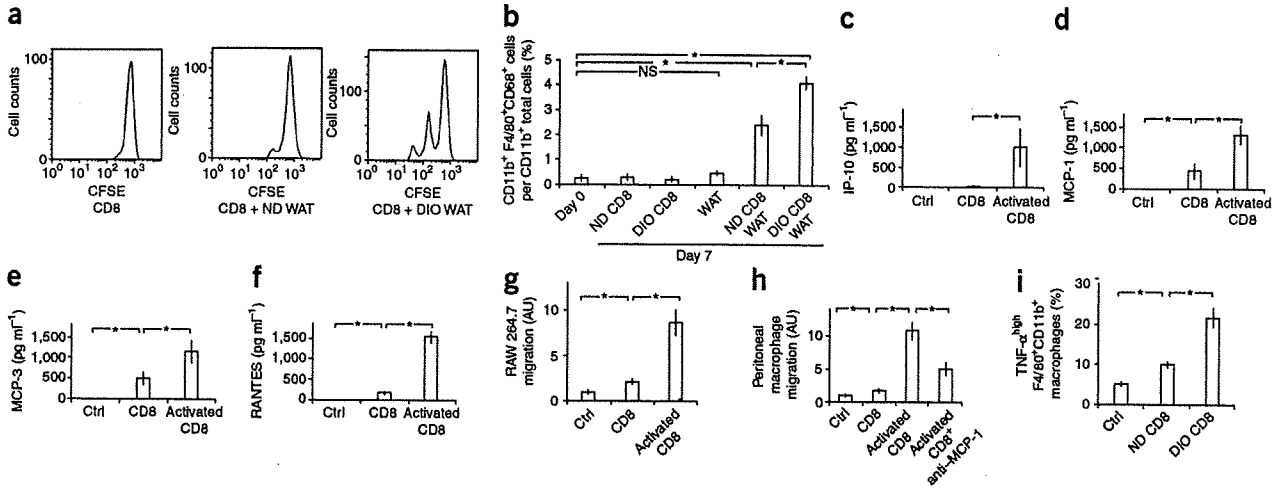

Figure 5 Interplay between macrophages, $CD8^+$ T cells and adipose tissue. (**a**) Carboxyfluorescein succinimidyl ester (CFSE) proliferation assay of isolated splenic $CD8^+$ T cells cultured with or without epididymal adipose tissue from ND or DIO mice. WAT, white adipose tissue. (**b**) Effects of $CD8^+$ T cells and adipose tissue on differentiation of peripheral blood monocytes ($CD11b^{high}Gr\text{-}1^-$) into macrophages ($CD11b^+F4/80^+CD68^+$). Monocytes were cocultured for 7 d with $CD8^+$ T cells isolated from epididymal adipose tissue from lean (ND CD8) or DIO (DIO CD8) mice, with or without epididymal WAT from lean mice. The differentiated macrophage fractions are shown ($n = 5$ in each group; $^*P < 0.05$; NS, not significant). (**c–f**) Concentrations of various cytokines in the control medium and medium conditioned by quiescent (CD8) or activated (activated CD8) CD8 cells ($n = 5$ in each group). $^*P < 0.05$. IP-10, interferon-inducible protein-10. (**g,h**) Migration of RAW264.7 (**g**) and peritoneal (**h**) macrophages, as examined using unconditioned control medium (Ctrl), medium conditioned by quiescent (CD8) or activated (activated CD8) $CD8^+$ T cells, or neutralizing antibody to MCP-1 (anti-MCP-1) ($n = 20$ in each group). $^*P < 0.05$. (**i**) The fraction of $F4/80^+$ $CD11b^+$ macrophages producing high levels of TNF-α after isolation from lean epididymal adipose tissue and cultured without (Ctrl) or with $CD8^+$ T cells isolated from ND (ND CD8) or DIO (DIO CD8) mice ($n = 5$ in each group, $^*P < 0.05$). Error bars represent means ± s.e.m.

migration, including interferon-inducible protein-10, monocyte chemoattractant protein-1 (MCP-1), MCP-3 and regulation upon activation, normal T cell expressed and secreted protein (RANTES) (**Fig. 5c–f**). When we plated cells of the macrophage cell line RAW264.7 or isolated peritoneal macrophages in Boyden chambers and treated them with medium conditioned by activated $CD8^+$ T cells, the numbers of both cell types that migrated through the pores between the chamber wells with activated $CD8^+$ T cell–conditioned medium were significantly higher compared to cells cultured in non-conditioned medium ($P < 0.05$ for each) (**Fig. 5g,h**). Treatment with antibody to MCP-1 lowered the migration of peritoneal macrophages by approximately half, indicating MCP-1 to be one of the factors mediating the humoral interactions (**Fig. 5h**).

To further assess the involvement of $CD8^+$ T cells in macrophage activation in adipose tissue, we cocultured $F4/80^+$ $CD11b^+$ macrophages isolated from lean epididymal fat tissue with $CD8^+$ cells isolated from either lean or obese fat tissue. The numbers of macrophages producing high amounts of TNF-α were significantly increased by the $CD8^+$ cells (**Fig. 5i**). Moreover, $CD8^+$ cells from obese adipose tissue increased the number of TNF-α^{high} macrophages to a significantly greater degree than those from lean adipose tissue (**Fig. 5i**). Collectively, then, the results of the coculture experiments show that the interaction between obese adipose tissue and $CD8^+$ T cells is crucial for macrophage differentiation, migration and activation.

DISCUSSION

Adipose tissue inflammation is now considered to be a crucial event leading to the metabolic syndrome, diabetes and atherosclerotic cardiovascular disease. However, it is still unclear how adipose inflammation is initiated and maintained. Here we showed that $CD8^+$ T cell infiltration precedes accumulation of macrophages in adipose tissue obesity, $CD8^+$ T cells are required for adipose tissue inflammation and $CD8^+$ T cells have major roles in macrophage differentiation, activation and migration. Thus, $CD8^+$ T cells are crucially involved in initiating inflammatory cascades in obese adipose tissue. Moreover, the finding that CD8-specific antibody treatment ameliorates preestablished adipose inflammation in DIO mice indicates that $CD8^+$ T cells are also essential for maintenance of the inflammatory response. Although infiltration of T cells into obese adipose tissue has been reported previously[10,18], to our knowledge, the present study is the first to directly address the functional role of $CD8^+$ cells in adipose tissue inflammation. The findings that systemic insulin resistance is ameliorated by CD8 depletion and aggravated by adoptive transfer of $CD8^+$ cells strongly suggest that CD8-dependent adipose inflammation has an impact on systemic metabolism.

Accumulation of $CD8^+$ T cells in obese epididymal fat pads was not accompanied by the presence of greater numbers of $CD8^+$ T cells in the systemic circulation, suggesting that $CD8^+$ T cells are activated by endogenous stimuli localized in the adipose tissue. Supporting this notion is our finding that obese adipose tissue induces $CD8^+$ T cell proliferation. The findings that incubation with $CD8^+$ T cells plus lean adipose tissue induced macrophage differentiation, although neither $CD8^+$ T cells nor lean adipose tissue did so alone, suggest that $CD8^+$ T cells and adipose tissue interact with each other to activate a local inflammatory cascade. In addition, the results of coculture experiments showing the interactions among $CD8^+$ T cells, macrophages and adipose tissue, as well as the results of our CD8 depletion experiments, which showed that $CD8^+$ T cells are essential for both the initiation and maintenance of adipose inflammation, strongly suggest that there is a relay involving both $CD8^+$ T cells and macrophages in obese adipose tissue that propagates local adipose inflammation.

In contrast to the increased infiltration of $CD8^+$ T cells, numbers of $CD4^+$ T cells and regulatory T cells were low at later time points (**Fig. 1**), which would also be expected to contribute to local inflammation within adipose tissue. For instance, subsets of $CD4^+$ T cells are known to secrete cytokines that can inhibit macrophage recruitment, including IL-4 and IL-10 (ref. 19), whereas regulatory T cells control adaptive immune responses by suppressing T cells, NK cells, NKT cells, B cells and dendritic cells[20]. In addition, regulatory T cells have also been shown to inhibit proinflammatory activation of monocytes[21] and to inhibit macrophage infiltration and renal injury in a model of chronic kidney disease[22]. It is therefore tempting to speculate that reducing the numbers of $CD4^+$ and regulatory T cells augments the inflammatory response during the late phase of adipose tissue obesity.

Taken together, our results support the idea that obese adipose tissue activates $CD8^+$ T cells, which, in turn, initiate and propagate inflammatory cascades, including the recruitment of monocytes and macrophages into obese adipose tissues and their subsequent differentiation and activation there. Thus, it seems that $CD8^+$ T cells have a primary role in obese adipose tissue inflammation, though future studies are needed to address which environmental cues within obese adipose tissue initiate $CD8^+$ cell infiltration. Even so, these results further support the idea that adipose inflammation has a major impact on systemic metabolism.

METHODS

Methods and any associated references are available in the online version of the paper at http://www.nature.com/naturemedicine/.

Note: Supplementary information is available on the Nature Medicine website.

ACKNOWLEDGMENTS

We gratefully acknowledge A. Matsuoka, X. Yingda, E. Magoshi, M. Hayashi, K. Wakabayashi, M. Tajima and Y. Yamazaki for excellent technical assistance. This study was supported by Research Fellowships from the Japan Society for the Promotion of Science for Young Scientists (S.N.), Grants-in-Aid for Scientific Research (I.M., R.N.) and grants for Translational Systems Biology and Medicine Initiative (R.N., T.K.) and Global Centers of Excellence program (R.N., T.K.) from the Ministry of Education, Culture, Sports, Science and Technology of Japan and a research grant from the National Institute of Biomedical Innovation (R.N.).

AUTHOR CONTRIBUTIONS

S.N. and M.N. performed *in vivo* and *in vitro* assays and analyzed all of the end points. K.H., K.U. and K.Y. performed human subject assays. S.N., I.M., K.E., H.Y., M. Otsu, M. Ohsugi, S.S., T.K. and R.N. supervised entire studies. S.N. and I.M. wrote the manuscript.

Published online at http://www.nature.com/naturemedicine/.
Reprints and permissions information is available online at http://npg.nature.com/reprintsandpermissions/.

1. Hotamisligil, G.S. Inflammation and metabolic disorders. *Nature* **444**, 860–867 (2006).
2. Weisberg, S.P. *et al.* Obesity is associated with macrophage accumulation in adipose tissue. *J. Clin. Invest.* **112**, 1796–1808 (2003).
3. Nishimura, S. *et al. In vivo* imaging in mice reveals local cell dynamics and inflammation in obese adipose tissue. *J. Clin. Invest.* **118**, 710–721 (2008).
4. Xu, H. *et al.* Chronic inflammation in fat plays a crucial role in the development of obesity-related insulin resistance. *J. Clin. Invest.* **112**, 1821–1830 (2003).
5. Savage, D.B., Petersen, K.F. & Shulman, G.I. Disordered lipid metabolism and the pathogenesis of insulin resistance. *Physiol. Rev.* **87**, 507–520 (2007).
6. Guilherme, A., Virbasius, J.V., Puri, V. & Czech, M.P. Adipocyte dysfunctions linking obesity to insulin resistance and type 2 diabetes. *Nat. Rev. Mol. Cell Biol.* **9**, 367–377 (2008).
7. Shoelson, S.E., Lee, J. & Goldfine, A.B. Inflammation and insulin resistance. *J. Clin. Invest.* **116**, 1793–1801 (2006).
8. Suganami, T., Nishida, J. & Ogawa, Y. A paracrine loop between adipocytes and macrophages aggravates inflammatory changes: role of free fatty acids and tumor necrosis factor alpha. *Arterioscler. Thromb. Vasc. Biol.* **25**, 2062–2068 (2005).

9. Wu, H. *et al.* T-cell accumulation and regulated on activation, normal T cell expressed and secreted upregulation in adipose tissue in obesity. *Circulation* **115**, 1029–1038 (2007).
10. Rausch, M.E., Weisberg, S., Vardhana, P. & Tortoriello, D.V. Obesity in C57BL/6J mice is characterized by adipose tissue hypoxia and cytotoxic T-cell infiltration. *Int. J. Obes. (Lond.)* **32**, 451–463 (2008).
11. Monney, L. *et al.* T_H1-specific cell surface protein Tim-3 regulates macrophage activation and severity of an autoimmune disease. *Nature* **415**, 536–541 (2002).
12. Brake, D.K., Smith, E.O., Mersmann, H., Smith, C.W. & Robker, R.L. ICAM-1 expression in adipose tissue: effects of diet-induced obesity in mice. *Am. J. Physiol. Cell Physiol.* **291**, C1232–C1239 (2006).
13. Traktuev, D.O. *et al.* A population of multipotent CD34-positive adipose stromal cells share pericyte and mesenchymal surface markers, reside in a periendothelial location and stabilize endothelial networks. *Circ. Res.* **102**, 77–85 (2008).
14. Nishimura, S. *et al.* Adipogenesis in obesity requires close interplay between differentiating adipocytes, stromal cells and blood vessels. *Diabetes* **56**, 1517–1526 (2007).
15. Cinti, S. *et al.* Adipocyte death defines macrophage localization and function in adipose tissue of obese mice and humans. *J. Lipid Res.* **46**, 2347–2355 (2005).
16. Sallusto, F., Lenig, D., Forster, R., Lipp, M. & Lanzavecchia, A. Two subsets of memory T lymphocytes with distinct homing potentials and effector functions. *Nature* **401**, 708–712 (1999).
17. Lumeng, C.N., Bodzin, J.L. & Saltiel, A.R. Obesity induces a phenotypic switch in adipose tissue macrophage polarization. *J. Clin. Invest.* **117**, 175–184 (2007).
18. Kintscher, U. *et al.* T-lymphocyte infiltration in visceral adipose tissue: a primary event in adipose tissue inflammation and the development of obesity-mediated insulin resistance. *Arterioscler. Thromb. Vasc. Biol.* **28**, 1304–1310 (2008).
19. Miller, R., Wen, X., Dunford, B., Wang, X. & Suzuki, Y. Cytokine production of $CD8^+$ immune T cells but not of $CD4^+$ T cells from *Toxoplasma gondii*–infected mice is polarized to a type 1 response following stimulation with tachyzoite-infected macrophages. *J. Interferon Cytokine Res.* **26**, 787–792 (2006).
20. Sakaguchi, S. *et al.* $Foxp3^+$ $CD25^+$ $CD4^+$ natural regulatory T cells in dominant self-tolerance and autoimmune disease. *Immunol. Rev.* **212**, 8–27 (2006).
21. Taams, L.S. *et al.* Modulation of monocyte/macrophage function by human $CD4^+CD25^+$ regulatory T cells. *Hum. Immunol.* **66**, 222–230 (2005).
22. Mahajan, D. *et al.* $CD4^+CD25^+$ regulatory T cells protect against injury in an innate murine model of chronic kidney disease. *J. Am. Soc. Nephrol.* **17**, 2731–2741 (2006).

ONLINE METHODS

Mice. We obtained Male C57BL/6J, *ob/ob* and *Cd8a*-deficient mice from Charles River Japan or Jackson Laboratories. All mice were housed under a 12-h light-dark cycle and allowed free access to food. To examine the time-course of changes in stromal vascular cell populations in adipose tissue under conditions of diet-induced obesity, we divided C57BL/6 mice into two groups and fed either a standard chow diet (6% fat, Oriental Yeast Company) or a high-fat diet (D12492, 60 Kcal% fat, Research Diets) from the age of 4 weeks.

To examine the effects of CD8 depletion on the initiation and development of adipose inflammation, we started antibody administration before the establishment of DIO. We fed male C57BL/6 mice a high-fat diet for 8 weeks, beginning when they were 4-weeks-old, and we intraperitoneally administered either CD8-specific antibody (3 μg per g body weight, 1 mg ml^{-1} solution, Biolegend) or control rat IgG (Sigma, 1 mg ml^{-1} PBS solution) weekly over the same period. We examined the mice at 12 weeks old (**Fig. 2** and **Supplementary Fig. 7**). We validated depletion of $CD8^+$ T cells by antibody as shown in **Supplementary Figure 11**.

To assess the effects of CD8 depletion on preestablished adipose inflammation in DIO mice, we fed C57BL/6 mice a high-fat diet, beginning when they were 9-weeks-old. Ten weeks later, we randomly assigned the 19-week-old obese mice to two groups and we intraperitoneally administered either CD8-specific antibody (120 μg per mouse) or control IgG three times per week for 2 weeks (total of six administrations). Age-matched lean C57BL/6 mice fed a normal chow diet served as controls. At 21 weeks, we performed oral glucose and insulin tolerance tests and then killed the mice for analysis of their adipose tissue (**Fig. 3** and **Supplementary Fig. 9**).

To assess the effects of CD8-deficient and adoptive transfer of $CD8^+$ T cells on adipose inflammation, we fed *CD8a*$^{-/-}$ mice either normal chow or a high-fat diet for 8 weeks, beginning when they were 6-weeks-old. We intravenously administered either 5×10^6 splenic $CD8^+$ T cells or control PBS weekly over the same period. We examined the *CD8a*$^{-/-}$ mice at 14-weeks-old. We prepared $CD8^+$ splenic T cells from 7-week-old C57BL/6 mice (**Fig. 4** and **Supplementary Fig. 10**). All experiments were approved by the Institutional Committee for Animal Research of The University of Tokyo and strictly adhered to the guidelines for animal experiments of The University of Tokyo.

Isolation of the stromal vascular fraction and flow cytometry. We isolated stromal vascular cells using previously described methods with some modifications. We killed the mice after general anesthesia after systemic heparinization. We removed the epididymal and subcutaneous adipose tissues and then minced it into small pieces (~2 mm). We vigorously agitated the pieces in PBS supplemented with 1 μg ml^{-1} heparin for 30 s to remove any circulating blood cells and then centrifuged the suspension at 1,000*g* for 8 min. We collected floating pieces of adipose tissue and incubated them for 20 min in collagenase solution (2 mg ml^{-1} of collagenase type 2 (Worthington) in Tyrode buffer (containing 137 mM NaCl, 5.4 mM KCl, 1.8 mM $CaCl_2$, 0.5 mM $MgCl_2$, 0.33 mM NaH_2PO_4, 5 mM HEPES and 5 mM glucose)) with gentle stirring. We then centrifuged the digested tissue again at 1,000*g* for 8 min. We resuspended the resultant pellet containing the stromal vascular fraction into PBS and filtered it through a 70-μm mesh. We washed the cells twice with PBS, incubated for 10 min in erythrocyte-lysing buffer (Becton Dickinson) as previously described[3], and we finally resuspended them in PBS supplemented with 3% FBS. We incubated these isolated cells with either labeled monoclonal antibody or isotype control antibody (eBioscience and BD Pharmingen) and analyzed by flow cytometry with a Vantage flow cytometer (Becton Dickinson) and FlowJo (Tree Star, Inc.) software. We used propidium iodide (Invitrogen) to exclude dead cells. We validated flow cytometric identification of M1 ($F4/80^+CD11c^+$) and M2 ($F4/80^+CD11c^-$) macrophages with CD11c markers as described in the **Supplementary Methods** and **Supplementary Figure 12**.

Immunohistochemistry. We stained and visualized whole-mount adipose tissue as previously described[14].

CFSE proliferation assay of $CD8^+$ T cells. We isolated splenic $CD8^+$ T cells from 7-week-old C57BL/6 mice and incubated the isolated $CD3^+$ $CD8^+$ cells with 5 μM CFSE (CellTrace CFSE Cell Proliferation Kit, Invitrogen). After staining, we incubated 2×10^5 cells in DMEM supplemented with 3% FBS for 2 d, with or without 20 mg of minced epididymal white adipose tissue prepared from either 20-week-old lean mice fed a normal chow diet or DIO mice fed a high-fat diet for 16 weeks. We harvested the $CD8^+$ cells and then analyzed them by flow cytometry to examine the proliferation status.

Differentiation of peripheral blood monocytes into macrophages. We isolated peripheral blood monocytes ($CD11b^{high}Gr\text{-}1^-$) from lean 7-week-old C57BL/6 mice. In the lower wells of a 24-well Multiwell Boyden chamber (Becton Dickinson), we cultured 5×10^4 monocytes per well in DMEM supplemented with 3% FBS, with or without 10 mg of minced epididymal adipose tissue prepared from 7-week-old lean mice in the upper wells. Also in the upper wells, we cultured 5×10^4 $CD3^+CD8^+CD4^-$ T cells, which we isolated from epididymal adipose tissues of 20-week-old lean or DIO mice. We incubated the cells for 7 d, after which the cells in the upper wells were collected, stained for CD11b, F4/80 and CD68, and assayed by flow cytometry for the differentiated macrophage fractions ($CD11b^+F4/80^+CD68^+$).

Migration of RAW264.7 and peritoneal macrophages. We isolated $CD8^+$ T cells from blood collected from C57BL/B6J mice after cardiac puncture. We isolated and cultured $CD3^+CD8^+$ cells were in DMEM supplemented with 3% FBS. To activate $CD8^+$ T cells, we cultured the cells with recombinant IL-2 (20 U ml^{-1}; Sigma), Dynabeads CD3/CD28 T Cell Expander (a bead-to-cell ratio of 1:1) and 2-mercaptoethanol (50 μM). After 120 h of culture, we aspirated the culture medium and performed migration assay using Boyden chambers with 8-μm pore inserts (Becton Dickinson). We cultured RAW264.7 and peritoneal macrophages in the upper wells, and we added the conditioned medium to the lower wells. We used fresh DMEM supplemented with 5% FBS as a control. To inhibit MCP-1 activity, we added a neutralizing antibody (5 μg ml^{-1} antibody to MCP-1, clone 2H5, Biolegend) to the conditioned medium.

TNF-α production in macrophages cocultured with $CD8^+$ cells. We isolated $F4/80^+$ $CD11b^+$ macrophages from epididymal adipose tissue from lean 7-week-old C57Bl/B6J mice, and we isolated $CD3^+CD8^+CD4^-$ T cells from epididymal adipose tissue from 20-week-old lean or DIO mice. We then added the adipose macrophages to the upper wells of a Multiwell Boyden chamber (Becton Dickinson) (5×10^4 cells per well), and we added the same number of $CD8^+$ T cells to the lower wells, after which we cultured the cells in DMEM supplemented with 3% FBS for 7 d. We assessed intracellular production of TNF-α by flow cytometry using an intracellular cytokine production detection kit (Cytofix/Cytoperm Fixation/Permeabilization Solution Kit, BD Pharmingen).

Human subjects. We acquired subcutaneous adipose tissue from healthy female donors undergoing liposuction of the abdomen or thighs (after obtaining their consent). We examined expression of *CD8a* in the tissue. We processed samples comprised of 1 g of each specimen by digestion with collagenase and then centrifuged to isolate the stromal vascular fractions. We purified total RNA using Trizol (Invitrogen) and determined relative mRNA levels using real-time PCR. This study was approved by the Ethics Committee of The University of Tokyo Hospital.

Statistical analyses. We expressed the results as means ± s.e.m. We determined the statistical significance of differences between two groups using Student's *t* tests, and we evaluated differences among three groups by analysis of variance followed by *post-hoc* Bonferroni tests. Values of $P < 0.05$ were considered significant.

Original Paper

Influence of Risk Factors for Metabolic Syndrome and Non-Alcoholic Fatty Liver Disease on the Progression and Prognosis of Hepatocellular Carcinoma

Susumu Takamatsu MD, PhD[1], Norio Noguchi MD, PhD[1], Atsushi Kudoh MD, PhD[1]
Noriaki Nakamura MD, PhD[1], Tohru Kawamura MD, PhD[1], Kenichi Teramoto MD, PhD[1]
Tohru Igari MD, PhD[2], and Shigeki Arii MD, PhD[1]

[1]Department of Hepato-biliary-pancreatic Surgery, Tokyo Medical and Dental University Graduate School of Medicine, and [2]Division of Pathology, Tokyo Medical and Dental University Hospital Faculty of Medicine, Tokyo, Japan

Corresponding Author: Susumu Takamatsu, MD, PhD, Department of Hepato-biliary-pancreatic Surgery Tokyo Medical and Dental University, Graduate School of Medicine, 1-5-45 Yushima, Bunkyo-ku, Tokyo 113-8519, Japan

Tel: +81 3 5803 5255, Fax: +81 3 3817 4126, E-mail: s.takamatsu@mac.com

ABSTRACT

Background/Aims: We investigated a relationship between the risk factors for metabolic syndrome, such as obesity, diabetes mellitus, hypertension, and hyperlipidemia, and the pathogenesis and outcome of hepatocellular carcinoma (HCC).

Methodology: One hundred twenty four patients who underwent curative resections for HCC were classified into 3 groups: those patients who were positive for hepatitis B surface antigen (group B), those positive for antibody to hepatitis C virus (group C), and those negative for both of them (non-B non-C) (group NBNC). The preoperative laboratory data, risk factors for metabolic syndrome, history of alcohol abuse, and outcome after surgery were investigated. The presence of non-alcoholic steatohepatitis (NASH) was also evaluated.

Results: The incidence of diabetes mellitus, hyperlipidemia, and alcohol abuse, and the serum level of triglyceride were significantly higher in group NBNC than in groups B or C. The risk factors for metabolic syndrome tended to lower the survival rates in group B and C, but not in group NBNC. Three of the 37 non-B non-C patients were associated with NASH.

Conclusions: It is suggested that the pathogenesis of non-B non-C HCC may be more closely associated with the risk factors for metabolic syndrome than that of hepatitis virus related HCC.

KEY WORDS: Hepatocellular carcinoma; Non-B non-C; Metabolic syndrome; Nonalcoholic steatohepatitis

ABBREVIATIONS: Hepatocellular Carcinoma (HCC); Hepatitis B Virus (HBV); Hepatitis C Virus (HCV); Hepatitis B Surface Antigen (HBsAg); Antibody Against HCV (HCVAb); Metabolic Syndrome (MS); Nonalcoholic Fatty-liver Disease (NAFLD); Nonalcoholic Steatohepatitis (NASH); Anibody Against Hepatitis B Surface Antigen (HBsAb); Antibody against Hepatitis B Core Antigen (HBcAb); Platelet Count (PLT); Asparate Aminotransferase (AST); Alanine Aminotransferase (ALT); Total *Cholesterol (TC); Triglyceride (TG);* Body Mass Index (BMI)

INTRODUCTION

Hepatocellular carcinoma (HCC) is one of the most common cancers, and its incidence has increased worldwide (1). Epidemiological studies and recent molecular biological investigations have revealed that hepatitis B virus (HBV) and hepatitis C virus (HCV) infection are major causes of HCC, and hence numerous basic and clinical studies have been conducted from the view point of hepatitis virus infection (1-6). On the other hand, little attention has been paid to HCC in patients without both hepatitis B surface antigen (HBsAg) and antibody against HCV (HCVAb), possibly because of the small population of these HCC patients (7-12). However, the number of HCC patients without apparent hepatitis virus infection has been increasing, and the so-called non-B non-C HCC has been the subject of investigation in recent years (10,11).

Recently, other factors such as obesity and type 2 diabetes mellitus, which were regarded as risk factors of metabolic syndrome (MS) (13), have been implicated in steatosis and fibrosis of the liver, and HCC (14-18). In addition, although the natural histories of non-alcoholic fatty-liver disease (NAFLD) or nonalcoholic steatohepatitis (NASH) have remained controversial, they have been considered to be one of the possible causes of cryptogenic cirrhosis of the liver and HCC (19-25). However, the relationship between HCC and NASH, as well as the incidence of HCC developing in the liver in response to NASH, has not been well understood. Moreover, the relationship between risk factors for MS, such as hyperlipidemia and hypertension, and HCC still remain unclear.

Based on this point of view, the present study investigated the participation of risk factors for MS in the pathogenesis and progression of HCC, and the outcome after surgical treatment. Evidence will be presented indicating that non-B non-C HCC is more closely related to those diseases with risk factors for MS than HCC associated hepatitis virus infection.

Hepato-Gastroenterology 2008; 55:609-614

METHODOLOGY

A total of 124 patients who underwent curative resections for HCC from April 2000 to March 2005 were enrolled in this study, and their medical records were reviewed retrospectively.

Twenty-six of the 124 patients had already undergone prior treatments including surgery, transcatheter arterial (chemo) embolization, and/or ablation therapy for HCC before being referred to our department.

The patients were divided into 3 groups: groups B, C, and NBNC. Those patients who were positive for HBsAg but negative for HCVAb were classified into the group B, and those who were negative for HBsAg but positive for HCVAb were classified as group C. The NBNC group was composed of the non-B non-C patients. In the non-B non-C patients, the antibody against hepatitis B surface antigen (HBsAb) and the antibody against hepatitis B core antigen (HBcAb) were also measured.

We examined the platelet count (PLT) and serum levels of asparate aminotransferase (AST), alanine aminotransferase (ALT), total cholesterol (TC), and triglyceride (TG) preoperatively. In addition, we investigated the body mass index (BMI), any history of alcohol abuse and risk factors for MS, which consisted of diabetes mellitus, hypertension, and hyperlipidemia (fasting plasma level of TC≥220mg/dL and/or TG≥150mg/dL), in each patient. All of the patients with diabetes mellitus and/or hypertension had already been diagnosed and treated before consulting us. Being overweight was defined as a BMI of 25kg/m^2 or more. A daily ethanol intake of 86g or more for 10 years was regarded as alcohol abuse.

The liver histology as well as the presence of NAFLD and NASH was evaluated in the resected specimens microscopically, especially in those patients without a history of alcohol consumption (daily alcohol intake within 20g) in the NBNC group. If there was moderate to severe macrovesicular steatosis, hepatocellular ballooning, lobular inflammation with necrosis of the hepatocytes and perisinusoidal fibrosis, we considered that NASH was present. The stage of the HCC was defined according to the Japanese general rules of primary liver cancer (26).

After surgical treatment, all of the patients were followed as out patients, and none of the patients underwent adjuvant therapies. Tumor markers such as alpha-fetoprotein and protein induced by vitamin K antagonist-II were measured every month, and ultrasonography, enhanced computed tomography, and/or magnetic resonance imaging were performed every 3 months. If an intrahepatic recurrence was suspected, computed tomography with angiography was performed to confirm.

We calculated the cumulative overall and disease free survival rates in each group, particularly for those patients with and without risk factors for MS.

The data are expressed as means ± standard deviation. Statistical analyses were performed by a one-way analysis of variance for parametric data, and by a Kruskal-Wallis test for categorical data among the three groups. If there was a significant difference on the Kruskal-Wallis test, a further analysis was performed by the Mann-Whitney test with Bonferroni's correction. Both the cumulative overall survival and disease free survival rates were calculated using the Kaplan-Meier method, and comparisons were made by using the log-rank test. A p-value of less than 0.05 was considered statistically significant.

TABLE 1 The Backgrounds of the 124 Patients

	B	C	NBNC	p
N	19	68	37	
Age	55.9±11.3	67.8±6.6	67.7±8.4	<0.0001[a]
Gender (Male/Female)	15 / 4	49 / 19	30 / 7	
Child-Pugh				N.S.
A	18	58	35	
B	1	10	1	
C	0	0	1	
Stage*				N.S.
I	1	13	2	
II	5	16	12	
III	7	27	17	
IVA	6	12	6	
Liver histology				0.03[b]
Normal liver	2	0	7	
Chronic hepatitis	8	31	17	
Liver cirrhosis	9	37	13	
Surgical procedure*				N.S.
Hr0	4	31	12	
HrS	8	14	8	
Hr1	2	12	9	
Hr2	5	10	8	
Hr3	0	1	0	
History of previous treatment	3	18	5	

*Stage and surgical procedure were defined according to the general rules for the clinical and pathological study of primary liver cancer, 4th edition. Hr 0: partial resection; Hr S: subsegmentectomy; Hr1: segmentectomy; Hr2: liver resection of 2 segments; Hr3: liver resection of 3 segments. N.S.: Not significant; [a]: B *vs.* NBNC and C; [b]: NBNC *vs.* C

TABLE 2 Preoperative Laboratory Data

	B	C	NBNC	p
AST (IU/L)	58.4±58.0	67.9±37.6	36.7±18.5	<0.001[a]
ALT (IU/L)	47.8±25.3	65.5±46.4	34.1±19.5	<0.001[b]
PLT (×104/mm^3)	15.5±5.5	13.7±7.7	19.6±12.2	<0.01[b]
Total Cholesterol (mg/dL)	174.0±46.3	152.1±35.9	180.1±39.1	<0.01[c]
Triglyceride (mg/dL)	76.0 ± 33.3	95.4 ± 43.9	138.3 ± 81.6	<0.001[a]

[a]: NBNC *vs.* B and C; [b]: NBNC *vs.* C; [c]: NBNC and B *vs.* C

TABLE 3 Associated Conditions

		B	C	NBNC	p
N		19	68	37	
Body Mass Index (kg/m^2)		22.0±3.1	22.8±3.2	24.1±4.1	N.S.
BMI ≥ 25	+/-	4 / 15	12 / 56	11 / 26	N.S.
Diabetes mellitus	+/-	1 / 18	15 / 53	17 / 20	<0 .01[a]
Hypertension	+/-	3 / 16	32 / 36	19 / 18	0.03[b]
Hyperlipidemia	+/-	3 / 16	11 / 57	14 / 23	0.03[c]
Alcohol abuse	+/-	6 / 13	13 / 55	16 / 21	0.03[c]

BMI: Body mass index; N.S.: Not significant; a: NBNC *vs.* B and C; [b]: B *vs.* NBNC and C; [c]: NBNC *vs.* C

RESULTS

Of the 124 patients, there were 94 men and 30 women, and the mean age was 65.9±9.0 years (range 30-82 years). The median postoperative follow-up period was 18.5 months (range 1-58 months).

The number of patients in groups B, C, and NBNC were 19 (15.3%), 68 (54.8%), and 37 (29.8%), respectively. In the NBNC patients, 17 (45.9%) of patients were positive for HBcAb and 16 patients were negative for HBcAb. Four patients were not examined for their HBsAb and/or HBcAb status. The background of these patients is summarized in Table 1. The mean age was significantly younger in group B than in groups C or NBNC ($p<0.0001$). The preoperative Child-Pugh scores were not significantly different among the 3 groups, but there was significant difference in liver histology ($p=0.03$); the incidence of chronic hepatitis and liver cirrhosis was significantly higher in group C than in groups B or NBNC. Both the stage of the HCC and the surgical procedure performed were decided based on the Japanese rules for HCC (26), and were not significantly different among the 3 groups.

Table 2 shows the preoperative laboratory data. Serum level of ALT was lower and the PLT was significantly higher in the NBNC group than in group C. The serum TG level was significantly higher in the NBNC group than in groups B or C.

The BMI and number of overweight patients were not significantly different among the three groups, as shown in Table 3. The frequency of diabetes mellitus was significantly higher in the NBNC group than in either group B or C. The incidences of both hyperlipidemia and alcohol abuse were significantly higher in the NBNC group as compared with group C.

Moreover, we made the same comparisons using those patients without alcohol abuse to exclude the influence of alcohol intake (Table 4). Consequently, we found that the laboratory data were not affected by alcohol abuse, whereas ratios of having associated conditions, such as diabetes mellitus, hyperlipidemia, and hypertension, became statistically insignificant among the 3 groups.

The cumulative overall survival rates at 1 and 3 years in groups B, C, and NBNC were 88.1% / 66.1%, 77.8% / 58.9%, and 85.5% / 69.8%, respectively (Figure 1). There were no significant differences among the three groups ($p=0.46$). The disease free survival rates at 1 and 3 years in groups B, C, and NBNC were 48.5% / 29.1%, 56.5% / 22.5%, and 73.8% / 27.6%, respectively (Figure 2). Although the NBNC group tended to be higher, the differences in the disease free survival rates among these three groups were not significant ($p=0.12$). In addition, to estimate the influence of risk factors for MS on survival after surgery, we compared the cumulative overall (Figure 3) and disease free (Figure 4) survival rates between those patients with *vs.* those without risk factors for MS in each group. In groups B and C, there was a trend that the survival rate was better in those patients without risk factors for MS. On the other hand, the survival rate was slightly better with risk factors for MS in the NBNC group. However, there were no significant differences between the groups. In groups B and C, the disease free survival rate was almost same with *vs.* without the risk factors for MS, and they were not significantly different in each group. In the NBNC group, the disease free survival seemed to be better in those patients with the risk factors for MS, but again there was no statistically significant difference ($p=0.24$).

Moreover, in the NBNC group, the overall ($p=0.50$) and disease free ($p=0.15$) survival rates were not significantly different between the two subgroups

TABLE 4 Laboratory Data, Liver Histology, and Associated Conditions in Patients without Alcohol Abuse

		B	C	NBNC	p
N		13	55	21	
AST (IU/L)		69.0±67.3	68.6±38.0	38.3±19.4	0.01[a]
ALT (IU/L)		52.6±27.1	63.9±45.3	39.0±21.5	< 0.05[b]
PLT ($\times 10^4$/mm^3)		16.3±6.5	13.1±7.9	21.6±14.0	< 0.01[b]
Total Cholesterol (mg/dL)		173.1±54.2	151.7±30.0	184.6±38.5	< 0.01[b]
Triglyceride (mg/dL)		76.4±34.6	95.3±39.4	124.1±69.7	< 0.05[a]
Liver histology					0.001[b]
Normal liver	1	0	5		
Chronic hepatitis	5	20	11		
Liver cirrhosis	7	35	5		
Diabetes mellitus	+/-	0 / 13	11 / 44	7 / 14	N.S.
Hypertension	+/-	3 / 10	27 / 28	9 / 12	N.S.
Hyperlipidemia	+/-	4 / 9	8 / 47	6 / 15	N.S.

N.S.: Not significant; [a]: NBNC *vs.* B and C; [b]: NBNC *vs.* C

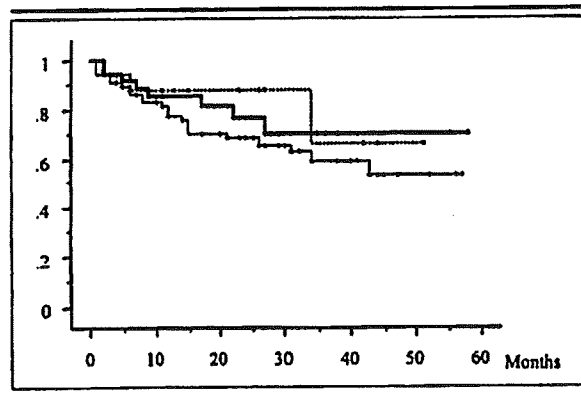

FIGURE 1
Cumulative overall survival curves for HCC after surgery. The bold line, dotted line, and thin line denote groups NBNC, B, and C, respectively. There were no significant differences in the overall survival rates among the 3 groups.

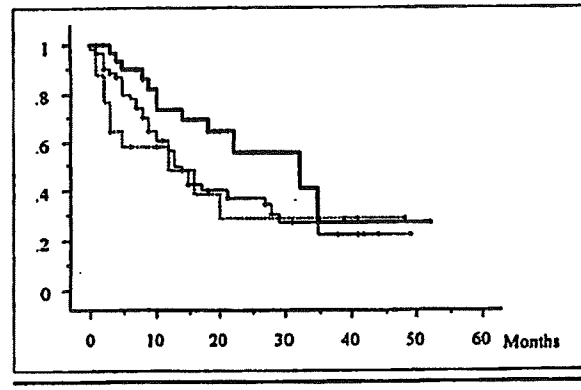

FIGURE 2
Disease-free survival curves for HCC after surgery. The bold line, dotted line, and thin line denote groups NBNC, B, and C, respectively. There were no significant differences in the disease-free survival rates among the 3 groups.